Sérgio Coelho, João Machado, Vítor Monteiro, João L. Afonso, "***Power Electronics Technologies for Renewable Energy Sources***", Book Chapter 11 in "Recent Advances in Renewable Energy Technologies", vol.2, 1st ed., Mejdi Jeguirim, Ed., Elsevier, 2022, pp.403-455, ISBN: 9780128235324, DOI 10.1016/B978-0-12-823532-4.00003-3.

Power Electronics Technologies for Renewable Energy Sources

Sergio Coelho, Joao Machado, Vitor Monteiro and Joao L. Afonso
University of Minho, Department of Industrial Electronics, Azurem, Guimaraes, Portugal

Abstract

Over the last decades, power grids are facing significant improvements mainly due to the integration of more and more technologies. In particular, renewable energy sources (RES) are contributing to moving from centralized energy production to a new paradigm of distributed energy production. Analyzing in more detail the requirements of the diverse technologies of RES, it is possible to identify a common and key point: power electronics. In fact, power electronics is the key technology to embrace the RES technologies towards controllability and the success of sustainability of power grids. In this context, this book chapter is focused on the analysis of diverse RES technologies from the point of view of power electronics, including the introduction and explanation of the operating principle of the most relevant RES, both in onshore and offshore scenarios. Additionally, are also presented the main topologies of power electronics converters used in the interface of RES.

1 Introduction

Over the last decades, climate changes have contributed significantly to the integration of more and more technologies into the power grid. Therefore, the paradigm of centralization energy production to a distributed production is an increasingly present reality. This is mainly due to the integration of distributed renewable energy sources (RES), which are seen as the main viable alternative to fossil fuels in the processes of generating electricity. Although the costs associated with RES are quite high, some governments have decided to invest in clean energy, mainly supported by solar photovoltaic and wind power systems. Such a measure is seen as a necessity due to environmental concerns, but also as a strategy that could bring long-term economic and political benefits [1], [2]. Over the last decades, thanks to the technological advances of RES, mainly solar photovoltaic and wind power systems, the efficiency of these systems increased and the costs, as expected, decreased. Although all the technological advances, fossil fuels for generating electricity remain a very accentuated reality, and it is necessary to develop new solutions and projects aiming to reduce CO_2 emissions to the atmosphere. In this sense, RES are seen as indispensable from an environmental point of view (also guaranteeing that technologies based on RES are clean) and considered essential to support the ever-increasing power demand.

In this context, the sustainability of the planet is a topic that has deserved special attention from society in general and from the scientific community. Regarding the more and more introduction of RES, both in large-scale and in micro-generation, an important challenge still is presented: the importance of new solutions of power electronics, both control algorithms and power converters, in the power production, transmission, and distribution [3]. The status and future outlooks of the power electronics as a key technology for RES are presented in [4] and issues related to the RES integration as a contribution for distributed generation are presented in [5]. For such purpose, consequently, it is fundamental to have power electronics with high efficiency and high reliability [6]. A survey about power electronics dedicated for the RES

integration is presented in [7] and the future perspectives of the energy systems with RES supported by power electronics are presented in [8]. Supported by dedicated control algorithms, power electronics are prepared to deal with the requirements imposed by the power grid and, at the same time, accomplishing the requirements of the end-users. A review of control algorithms dedicated to distributed generation is presented in [9]. In [10] are presented power electronics converters dedicated for the interface of photovoltaic and wind power systems with the power grid. In [11] is also presented a review specifically dedicated to power electronics converters interfacing photovoltaic systems with the power grid. A review of transformer-less power electronics topologies specifically dedicated to photovoltaic systems is presented in [12]. Specifically, regarding wind turbines, a review of power electronics converters is presented in [13] and future perspectives are presented in [14]. Supported by the vital demand of reliable and environmentally friendly power production from RES, its total production is constantly prosperous, and it is expected to a significant increase in the next few decades [15].

In this context, abundant efforts have been made by various countries with the objective to introduce more RES in on-grid and off-grid configuration, with a special preponderance for solar photovoltaic and wind power systems as the most promising technologies. Figure 1.1 shows a simple overview of interfacing RES in on-grid and off-grid configurations. Consequently, new possibilities, but also new problems can be introduced in the electric grid, being necessary that it is able to answer the energy needs of the consumers and, in addition, has the capacity to fill possible failures and power quality problems. Additionally, the increasing penetration of electric vehicles, energy storage systems and new controlled electrical appliances are also seen as new an opportunity, and a challenge for the RES introduction [16], [17]. In view of this change, power grids are also changing to introduce new paradigms, such as smart grids and smart homes. The objective is to make the power grid more sustainable, secure, and flexible, allowing the bidirectional transfer of power and information between all the systems. With the adoption of distributed generation systems, the reach and flexibility of the power grid are superior when compared to the current scenario, making the consumer also a power producer, i.e., a prosumer. RES, in addition to the impact on smart grids, have been used more frequently in the creation of off-grid systems in remote locations. RES has an intermittent profile, however, at any time of the day and regardless of atmospheric conditions, it is essential that the energy produced is the maximum, using, for this purpose, certain strategies and algorithms in power electronics systems. Even so, in addition to adverse atmospheric conditions, there are several factors that can limit or prevent the generation of energy through these sources. As a complement of traditional onshore power production from RES, the power generation using RES in an offshore regime has been gaining preponderance in the power generation mix [18], [19], since there are a large number of advantages when compared to the onshore regime, particularly in terms of atmospheric conditions (e.g., wind, temperature, radiation).

The main contribution of this book chapter relies on the analysis of the most diverse RES from the point of view of power electronics. In this sense, in section 2 is presented a short introduction and explanation of the operating principle of the most relevant RES, highlighting the main advantages and disadvantages of each one and presenting application cases. Section 3 discusses possible architectures for energy transmission and distribution systems, both onshore and offshore, supported by power electronics technologies. Moreover, this item also presents some topologies of power electronics converters used in the interface with the most diverse RES. Finally, in section 4, some conclusions are highlighted.

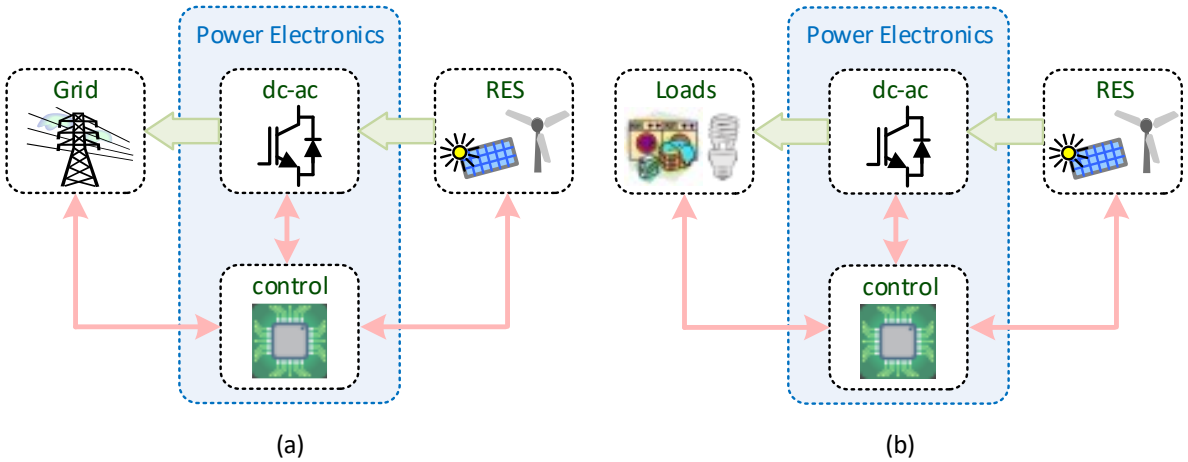

Figure 1.1. Integration of renewable energy sources (RES) considering:
(a) On-grid configuration; (b) Off-grid configuration.

2 Renewable Energy Sources

To achieve the carbon neutrality targets by the year 2050, it is essential, among other measures, that RES-based power generation methods continue to evolve gradually [20]. However, in addition to environmental issues, these generation systems must be considered economically viable, both for the consumer and for the energy producer. In addition, society needs to change its behavior regarding this issue, adopting energy rationalization strategies and increase the efficiency of the power electronics systems.

From the power electronics point of view, emerging technologies are being frequently employed in RES-based power generation systems, as well as new control algorithms and topologies that intend to increase their efficiency. Consequently, business competitiveness will also increase, the reason why the energy mix is fairly different between each country. Although different, the biggest contributors to the energy mix of each country are, in general, hydropower, wind and solar PV. Even so, geothermal, biomass, and marine power (waves, tidal, temperature gradient, and salinity gradient power) are also considered [20].

In this respect,

Table 2.*1* presents a comparative study between the electric power production of some EU countries in the years 2005 and 2018. It is also analyzed the percentage that RES represents in the total energy mix of each country, denoting a marked growth in almost all countries over these 13 years. Note that EU countries that are not represented in

Table 2.*1* have a percentage of RES-based electric power production below 20% in 2018.

In the case of Portugal, it is verified that, in 2018, RES accounted for more than half of the total energy produced in the country (51.6 %). This situation is, once again, represented in Table 2.2 and in Figure 2.1, in which the contribution of each renewable to the annual production of electricity based on RES in Portugal is presented, this time between the years 2011 and 2019. However, it should also be noted that the total annual production does not include the water pumping component, which, e.g., was accounted for at 1235 GWh in the year 2018 and at 1425 GWh in 2019 [21].

In this respect, the following items present each of the aforementioned RES, explaining the process of energy generation and analyzing some of the frequently used technologies.

Table 2.1-Electrical energy production in EU countries.

	2005			2018			
	Total (TWh)	RES (TWh)	%RES	Total (TWh)	RES (TWh)	%RES	%RES increase
Austria	69.4	40.9	58.9	77.5	50	64.5	+5.6
Sweden	151.0	81.2	53.8	146.2	91.1	62.4	+8.6
Denmark	37.6	9.8	26.1	35.6	20.8	58.3	+32.2
Portugal	53.4	8.3	15.5	57.0	29.4	51.6	+36.1
Croatia	17.6	7.1	40.2	19.0	9.8	51.4	+11.2
Latvia	7.1	3.4	48.4	7.6	3.5	45.8	-2.6
Romania	56.5	20.2	35.8	62.3	26.2	42.0	+6.2
Germany	615.5	63.4	10.3	592.8	224.7	37.9	+27.6
Spain	287.7	42.3	14.7	285.4	103.9	36.4	+21.7
Finland	87.3	23.5	26.9	89.9	32.1	35.7	+8.8
Italy	351.7	48.4	13.8	332.9	114.4	34.4	+20.6
Slovenia	14.8	3.6	24.2	15.8	5.2	33.1	+8.9
Ireland	28.0	1.9	6.7	31.1	10.2	32.8	+26.1
Greece	63.8	6.4	10.0	59.5	16.1	27.1	+17.1
Bulgaria	36.8	4.3	11.7	39	9.3	23.8	+12.1
France	515.6	56.3	10.9	518.2	113.4	21.9	+11.0

Table 2.2-Annual production of electric energy based on RES in Portugal between 2011 and 2019 (GWh).

	2011	2012	2013	2014	2015	2016	2017	2018	2019
Hydro	11536	5622	13730	15569	8661	15730	5897	12393	8818
Wind	9162	10260	12015	12111	11608	12474	12248	12617	13667
Biomass	2467	2496	2516	2578	2518	2481	2573	2558	2749
Urban Solid Waste (USW)	296	245	286	240	292	305	360	327	349
Biogas	161	210	250	278	294	285	287	271	264
Geothermal	210	146	197	205	204	172	217	230	215
Solar PV	282	393	479	627	799	871	993	1006	1342
Total	24114	19372	29473	31610	24375	32317	22574	29402	27405

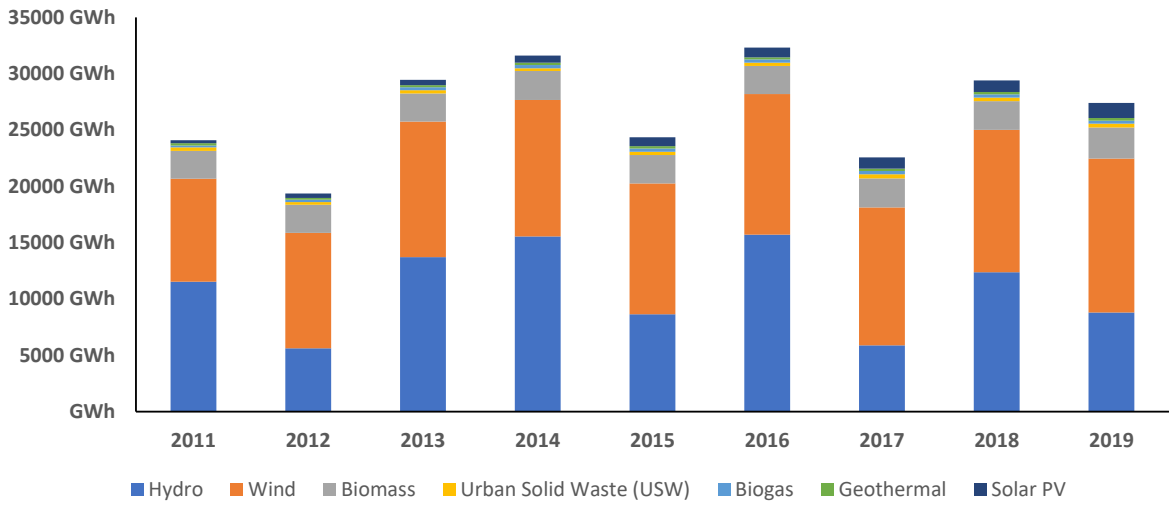

Figure 2.1. Annual production of electrical energy based on RES in Portugal between 2011 and 2019.

2.1 Hydropower

In the case of hydropower, electricity is produced based on the rotating motion of a turbine coupled to a generator, an action caused by the force and/or movement of a body of water. Thus, the kinetic energy of a water stream or the potential energy of water stored in a reservoir at altitude is used to promote the described rotational movement. In this respect, two main types of hydroelectric power plants are highlighted: run-of-river and reservoir.

That said, the major difference between the two types of hydroelectric power plants lies, fundamentally, in the method of generating electric power. On one hand, run-of-river plants present lower or no water storage capacity, being the kinetic energy of the river current that rotates the turbine. In turn, reservoir plants, as the name suggests, store large amounts of water in the form of potential energy, thus rotating the generator axis due to the action of the gravity force. In this respect, considering the aforementioned differences, it is possible to conclude that reservoir power plants are endowed with water flow control capacity, which is not the case with run-of-river plants since they depend on the seasonal levels of the river [22].

Some reservoir power plants are capable of re-storing water, pumping it in the reverse direction, i.e., from a downstream reservoir (only existing in this type of plant) to a bigger one upstream the dam, a method that is named pumped-storage hydroelectricity or pumped hydroelectric energy storage. At first sight, this feature makes the hydroelectric plant an energy-consuming element, however, the system contributes to level consumption and production profiles of energy [23]. When there is a production surplus, the power is used to pump water to the upper reservoir. In this way, it is possible to generate, once again, electricity during grid peak periods. From another perspective, this type of hydroelectric power plant facilitates the integration of renewables into the power grid. Since RES has an intermittent power production, as is the case of wind or solar PV, the production of electric power based on these, is, sometimes, carried out during off-peak periods. This surplus of energy should be, as an optimum solution, stored in batteries or any other type of energy storage system. Thus, pumped-storage plants are considered a viable solution since the excess of energy produced by these intermittent RES can be used, once again, to store water in the form of potential energy [24].

Nowadays, hydropower is seen as one of the main alternatives to the burning of fossil fuels for the production of electricity, not only in Portugal but worldwide. Moreover, hydroelectric plants are highly efficient, actively contribute to the grid stabilization, in certain regions are capable of enhancing economic activities and generating employment, and, as aforementioned, some of them have the capacity to store water in the form of potential energy.

On the other hand, the implementation of a hydroelectric power plant can cause a negative effect on the environment, which is considered lower in run-of-river stations when compared to reservoir ones. That said, it is observed, in some cases, soil erosion, alteration of the river flow, and an increase in the evaporation area, directly influencing ecosystems. Therefore, according to the magnitude of the project, the construction of a dam can also cause the displacement of populations [22]. Obviously, to minimize these risks, studies must be performed, and preventive measures must be taken during the project.

2.2 Wind Power

Wind power has gained greater preponderance in the international energy mix after the 1970's oil crisis, but its origin is much more remote. The electricity produced based on this RES results, even if indirectly, from the rotation of a turbine through the force of the wind.

However, considering certain parameters such as wind speed or the implementation site of the system, wind turbines are considered horizontal axis or vertical axis. Notwithstanding, for both cases, the wind flows through the turbine blades and rotor (blade fixation system), transforming kinetic energy into rotational mechanical power. In turn, the rotor is coupled to a low-speed shaft that, by the action of a gearbox, rotates the central axis of a generator at a higher speed.

Since wind speed is not constant throughout the day, it is necessary to employ control algorithms and mechanical or software limitations to avoid possible damage to the wind turbines. Furthermore, the wind speed is also associated with the power values produced, and as expected, the latter need to be controlled, regulating, to this end, the parcel of kinetic energy that is transformed into mechanical power. Among power control regulation methods, passive stall, active stall, and pitch techniques stand out. The main difference between these three techniques lies in the way that the turbines counter wind speed when it is excessive.

In the case of a wind turbines with passive stall control, it is the fixed geometry of the blade that makes it less aerodynamic when the wind speed reaches a certain value, even decreasing the rotor rotation speed. However, this technique is mechanically limiting and less efficient, the reason why active stall control is more commonly used. In this technique, after the wind speed reaches a determined critical value, the shape and geometry of the turbine blades vary. At that moment, speed brakes are deployed, a mechanism that adds drag to the blades and, consequently, less speed and power. On the other hand, pitch control is considered an active and mechanical process, in which the electronic controller of the turbine is constantly reading the output power values that are produced. When the power is too high, each of the turbine blades pitches (turns) longitudinally out of the wind, slowing down the rotor. Conversely, when the wind speed decreases, the blades return dynamically to their initial position [25].

Notwithstanding, only a fraction of the wind kinetic energy (C_p) is transformed into mechanical power (P_o, expressed by (2.1)), as Betz's Law states. According to this Law, only 59% of the wind power is captured by the rotor blades, whereas the remaining percentage is discharged or wasted. Thus, the maximum power extracted from the wind (P_{max}) is given by (2.2), where ρ is the air density (kg/m^3), A is the swept area of the rotor blades (m^2) and V is the velocity of the air (m/s).

$$P_o = \frac{1}{2}\,\rho\,A\,V^3\,C_p \tag{2.1}$$

$$P_{max} = \frac{1}{2}\,\rho\,A\,V^3\,0.59 \tag{2.2}$$

However, wind turbines typically present a C_p value below 50%, slightly lower than what is stated (59%). This difference is justified according to mechanical losses, thus reducing the fraction of maximum power that can be generated. In this regard, assuming a value of 0.5 for C_p, P_{max} can be expressed by:

$$P_{max} = \frac{1}{4}\,\rho\,A\,V^3 \tag{2.3}$$

In turn, the value of A varies according to the type of turbine. For a horizontal axis turbine, A is dependent on the rotor diameter (D) and expressed in (2.4). The determination of A can be considered complex for other types of turbines, assuming, in most cases, parabolic curves.

$$A = \frac{\pi}{4}\,D^2 \tag{2.4}$$

On the negative side, wind-based generation technology enhances noise pollution and can be responsible for an aggravated impact on fauna and flora [26].

Regarding offshore generation systems, wind power is considered the most developed and consolidated. The efficiency of this technology is superior when compared to the onshore regime since wind speed is higher and the absence of physical barriers means that its intensity is practically constant. Nowadays, offshore wind farms are located in shallow waters and relatively far from the coast, as well as outside maritime traffic routes, strategic naval facilities, and spaces of ecological interest. Thus, the visual and acoustic impact is reduced, allowing the installation of large structures and plants with hundreds of MW, which rarely happens on land.

In Portugal, Windfloat Atlantic is a pioneering project with a worldwide dimension, referring to the first floating offshore wind farm. This structure is composed of 3 turbines and has a total installed power capacity of 25 MW. Windfloat Atlantic has opened a new horizon for offshore wind power, validating the installation of wind turbines in deeper waters. In this respect, it is common practice that in shallow waters a cement base, tripod or quadropod, and mono-pillar structures are used, whereas, in deeper waters, jacket, spar-buoy, and submersible structures are employed.

2.3 Solar Power

The photovoltaic effect is the physical and chemical phenomenon responsible for converting solar radiation into voltage and electric current in the terminals of a semiconductor material. Photons are the particles that transport energy from the solar radiation and, at the moment of their incidence on the surface of a solar PV module, are absorbed by solar PV cells. The latter is the element that converts the solar radiation into electric power, however, it is imposed the need to associate them in series and/or parallel in order to increase the voltage and current values produced by the solar PV module. In this respect, the aggregation of several cells constitutes a module that, also when associated with each other, makes up a solar PV panel. Unlike cells, that present a brittle and fragile structure, a solar PV panel has greater robustness in the face of atmospheric conditions, thus avoiding the corrosion of electrical contacts and the existence of possible short-circuits.

Thus, to generate an electric potential in each solar PV cell, the latter must be based on a conductive material which, in most cases, is silicon. When a photon is absorbed by the cell, its energy is transferred to the electrons of the silicon atoms, causing its stimulation and movement along the semiconductor layers of the cell (P-N junction). This constant movement of particles generates an electric potential between the semiconductor layers and, consequently, a dc current. However, the maximum power produced by a solar PV panel is dependent on several external factors, such as ambient temperature, incident radiation, and maintenance frequency.

Due to its ease of installation and low maintenance costs, solar PV is the most commonly used RES-based generation technology in low power systems, e.g., self-consumption production units. However, since the energy efficiency of the panel depends on the semiconductor material for the cells, such costs are also directly associated with this choice. Obviously, solar PV panels with greater efficiency are normally more expensive and, therefore, used in very specific applications and in large power plants. On the other hand, in, e.g., self-consumption units, the main concern is to make its acquisition economically viable.

Given that the implementation space for large solar PV power plants in onshore regimes is more limited, over the last decade, solar offshore projects. i.e., floating PV technology began to be studied and implemented worldwide. The layout of this technology is analogous to a terrestrial solar PV system, only differentiating the fixation structure of the PV panels [27]. In

any floating PV system, there are specific fixation and floating systems, as well as an underwater cable that transmits the produced power to land. In the majority of the cases, solar PV panels are placed with fixed inclination using pontoon floats, whether they are pure floats or floats combined with metal trusses. The floating platform is fixed with an anchoring and mooring system, either to the seabed or using pillars or a bench (also, the three fixation types can be combined). As for the implementation site, floating PV systems are normally installed in drinking water reservoirs or basins, lakes, etc.

Floating PV systems present several advantages in comparison with traditional onshore installations, highlighting the profitability of aquatic spaces not "occupied" until then. Moreover, solar PV panels present greater efficiency in these locations since their structure is in direct contact with water, thus lowering the temperature. Due to the fact that the structure creates shade on the water surface, the level of water evaporation is reduced, which, in regions with the scarcity of this resource, is considered an excellent benefit. Finally, in order to not create new power transport technologies, they can be used, e.g., those of an existing hydroelectric power plant, thus rationalizing resources. In turn, since floating PV power generation is only carried out on large scale, accommodating a great number of modules and complementary equipment, the size of the plant and the costs are much higher. Most importantly, it should also be noted that solar floating PV technology has been growing in terms of projects and prototypes worldwide, although not as fast as intended [27], [28].

Solar radiance, in addition to the solar PV component, can also be used via solar thermal energy, commonly named concentrating solar power (CSP). Among its purposes, the production of electrical power and the heating of water stand out. As the name suggests, throughout the power generation process, there are utilized systems that concentrate the radiance into an absorbing cavity, thus allowing to heat a fluid (water, oil, etc.). This same fluid is posteriorly used in a "conventional thermodynamical" cycle, in everything analogous to fossil fuel thermoelectric plants, in which steam is used to rotate a turbine and produce electric power [29].

Despite the technological advances verified over the last decades, CSP is relatively recent, the reason why it is still in a much lower phase when compared with, e.g., solar PV or wind power.

2.4 Other Renewable Power Generation Methods

Biomass is the term that defines renewable energy products generated from organic matter. From the point of view of electric power production, this RES consists of the total amount of organic matter in an ecosystem, either plant or animal originated. There are determined processes that lead to the use of biomass as a source of several forms of energy. In this sense, they are divided into three main groups: thermochemical processes, biological processes, and direct combustion processes. Thermochemical processes are based on a heat source to transform the biomass, whereas biological methods utilize several microorganisms to decompose biomass, a characteristic that provides higher energy value to this resource [30], [31].

Geothermal power is based on the transformation of the existing heat inside the earth and it is considered one of the cleanest and most reliable types of energy. The earth's heat can be used for electric power generation, for indirect use (e.g., thermal baths, industry, etc.), or also for heating, through geothermal heat pumps. Considering some factors such as temperature (oscillating between 75°C and 300°C), depth, and extracted steam, three types of geothermal power plants are considered: dry steam, flash steam, and binary cycle [32]–[34].

As know, the seas and oceans provide several possibilities and mechanisms for the generation of electrical power. Regarding maritime power, waves are considered the result of

the wind force acting on the water surface, being their size influenced by the intensity and speed of the wind, the time it blows in the same direction, the topography and depth of the seafloor, and by the length of the active area without obstacles. Regarding power generation methods, wave energy converters are classified as: (i) Oscillating water column; (ii) Overtopping devices; (iii) Oscillating devices [32], [35]–[37].

Tides are caused by astronomical phenomena related to the gravitational force exerted by the moon and the sun on the earth but, also meteorological and geological factors at a given location contribute to its appearance. One of the power generating methods is named tidal barrage, in which electricity is produced both during high and low tides (single-effect mode), taking advantage of the potential energy in the height difference between the tides, or even combining the two variants (double-effect mode). On the other hand, the tidal stream generation method is based on the transformation of the kinetic energy of the water currents. In this respect, several technologies are considered for the kinetic energy transformation method, thus highlighting vertical axis turbine, oscillating hydrofoil, venturi effect devices, Archimedes screw, and tidal kite [32], [38].

Salinity gradient power is another maritime technique for generating electricity, having, as an operating principle, the difference in salt concentration between two fluids. Such salinity difference can be obtained when freshwater from a river flows into the ocean, however, other types of fluids or situations are equally valid. Although there are several ways to produce electrical power based on this RES, only two of them are in development at the commercial level: pressure retarded osmosis and reverse electro-dialysis. In both processes are used membranes, a component that assumes a critical role in the system operation [39].

The ocean thermal energy conversion is based on the temperature difference of the ocean water. The surface water, due to presenting higher temperature, is used to generate steam, either through a vacuum chamber or by thermal transfer to a fluid with a boiling point lower than the one of water. On the other hand, to consider this generation method profitable, the differential temperature must be at least 20°C, which constitutes a major drawback. Ocean thermal energy generation systems may operate in closed-cycle, open-cycle, or in a hybrid structure [40]–[43].

3 Power Electronics Converters for Renewable Energy Sources

As mentioned in the introduction of this book chapter, power electronics play a central role in the growing dissemination of power generation systems based on RES, both in large power plants and, e.g., in self-consumption production units. Thus, this item introduces the main power electronics topologies for the interface of each of the aforementioned renewable, namely isolated and non-isolated converters, multilevel and interleaved architectures, and single-phase and three-phase converters.

3.1 Turbine-based Power Systems

In power generation systems based on the transformation of mechanical energy using turbines and generators, e.g., wind power, hydropower, etc., topologies of power converters and control algorithms capable of realizing an intelligent interface between the RES and the power grid (or certain electrical appliances) must be adopted. Among other aspects, the efficiency of these generation technologies is also influenced by the blade rotational speed, torque, and frequency, which vary according to the characteristics of the generation system. The power grid interface must, therefore, obey to certain parameters in order to do not compromise its stability. On the other hand, the power supplied to the consumer must respect determined regulated

quality standards, which include frequency adjustment, active power control, reactive power control (to regulate power grid voltage), fault tolerance, protection and the mitigation of power quality problems, as it the case of flickers, harmonics and voltage and current fluctuation.

In the early years after the dissemination of power generation technologies based on the action of the wind, water, or steam, asynchronous generators (induction) were used to interface the power grid since they were (and still are) a brushless technology (in the case of squirrel cage rotors), reliable, cheap, lightweight, low maintenance, and widely available in the market. However, considering the technological evolution in the field of power electronics (power semiconductors, etc.), new configurations and methods have emerged, and, among other changes, synchronous generators began to be used, both wound rotor and permanent magnet. Thus, it is possible to, e.g., rectify oscillations in the values of power produced since the asynchronous generator is directly connected to the power grid, thus operating at a fixed speed.

3.1.1 Wind Turbines

Highlighting wind power, the rotation speed of the turbines and the central axis of the generator can be variable or fixed, thus, four types of speed control are considered: (i) Fixed speed; (ii) Partial variable speed; (iii) Variable speed with partial-scale frequency converter; (iv) Variable speed with full-scale power converter [44].

In the case of fixed wind speed turbines, the induction motor is connected to the blades via a gearbox and to the power grid via a step-up transformer. Therefore, since a squirrel cage induction generator is considered, there is a need to absorb reactive power from the power grid so that the electromagnetic field necessary for the conversion of mechanical energy into electrical power is established through the stator. Thus, to compensate for such reactive power values, a capacitor bank must be introduced, as shown in Figure 3.1. On the other hand, the introduction of a soft starter in this configuration is justified by the fact that the induction motor requires a high initial magnetization current, which can be a synonym of problems for the power grid. Although commercial solutions for fixed speed wind turbines still exist, this architecture has fallen into disuse due to its significant disadvantages. As examples are highlighted lower wind energy conversion efficiency, changes in the wind speed are reflected in the power grid, and severe stress on the mechanical components can occur due to grid faults.

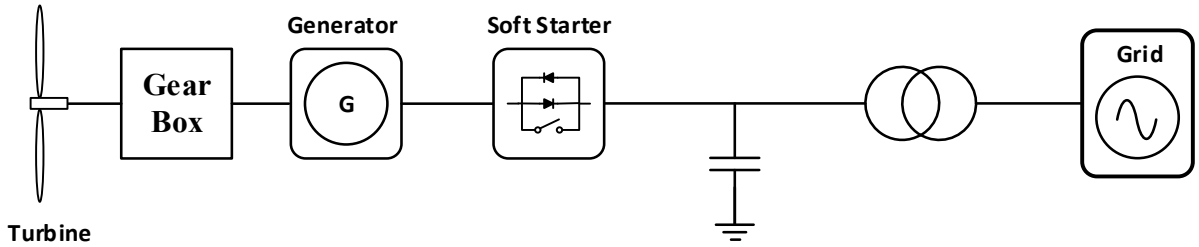

Figure 3.1. Fixed-speed wind turbines.

In turn, in the case of partial variable speed wind turbines, the stator of a wound rotor induction generator is connected to the power grid via a transformer, reactive power compensation is performed with the aid of a capacitor bank, and a soft starter is considered for the sake of initial magnetization current limiting purposes. However, when in comparison with fixed speed wind turbines, the difference is related to the fact that the rotor of the generator is connected to a variable resistor, as can be observed in Figure 3.2. The latter is easily adjustable and has a direct impact on the slip value, thus changing the rotational speed in accordance. Depending on the value of the resistor, the speed range oscillates between 0% and 10% above the synchronism speed of the generator. This alteration allows to increase the energy

conversion efficiency and reduce the mechanical stress in the gearbox and bearings, thus increasing its lifecycle.

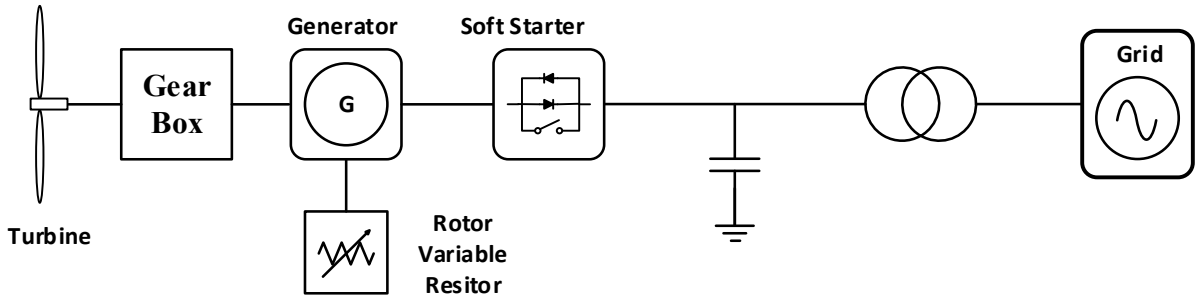

Figure 3.2. Partial variable speed wind turbines.

Variable speed wind turbines with a partial-scale frequency converter are constituted by a gearbox, a step-up transformer, a wound rotor induction generator, and an ac-dc-ac converter topology connected to the rotor terminal, as can be seen in Figure 3.3. However, since the stator is directly connected to the power grid (commonly, by a 3-phase transformer), this configuration is also known as a doubly-fed induction generator. Contrary to the aforementioned types of speed control wind turbines, reactive power compensation is now ensured by the ac-dc-ac converter, as well as the generator soft start. With the connection of the ac-dc-ac converter to the rotor, it is possible to increase the speed range, this time from -30% to 30% above the synchronous speed, thus verifying a bidirectional power flow in the rotor circuit. Additionally, with the adoption of an MPPT control technique, it is also possible to increase the power conversion efficiency and the robustness of the system. Notwithstanding, the main drawbacks are high maintenance costs and the decrease in the lifetime of some components. As an example, due to the fact that the ac-dc-ac power converter is connected to the rotor using brushes and rings, i.e., equipment with rapid wear, maintenance must be performed regularly, increasing the costs. Such a characteristic precludes this configuration from being employed in offshore wind turbines, where maintenance and travel costs would be much higher.

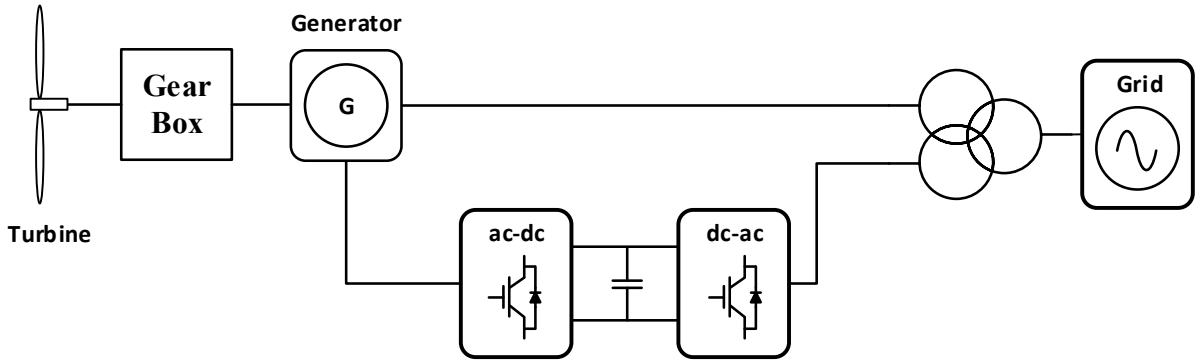

Figure 3.3. Variable speed wind turbines with a partial-scale frequency converter.

On the other hand, for variable speed wind turbines with a full-scale power converter, it is possible to increase the speed range of the generator up to 100%. This operating characteristic is obtained by connecting an ac-dc-ac power converter between the stator of the generator and the step-up transformer, thus establishing the interface with the power grid, as shown in Figure 3.4. Moreover, the reactive power compensation and the soft start are ensured, once again, by the ac-dc-ac power converter. However, contrarily to the aforementioned cases, synchronous generators may also be adopted, namely wound rotor synchronous generator and permanent magnet synchronous generator. In this sense, if a synchronous generator with a high number of poles is selected, the need for the gearbox can be excluded. Besides the gearbox, also rings and brushes can be eliminated in the case of the use of a permanent magnet generator,

thus simplifying the design and allowing to reduce the costs and the maintenance frequency. In this respect, and as its name indicates, the excitation of this type of synchronous generator is carried out using magnets and not electrically.

As already mentioned, the adoption of wound rotor synchronous generators in wind turbines has become an increasingly frequent practice. However, due to its own operating characteristics, its electrical excitation must be controlled with the aid of variable resistors or power converters based on thyristors or fully controlled semiconductors (e.g., IGBT or MOSFET). Thus, the power grid interface can be directly established or using an ac-dc-ac power converter. This converter stage, considering the power values produced by the wind turbines, may present different topologies. Thus, for low power systems, two-level voltage source converters (2L-VSC) in a back-to-back regime (sharing a dc-link) are often used, as shown in Figure 3.5. However, this topology presents, as the main drawback, high semiconductor stress, justified by the fact that the current that flows through them is also high. Alternatively, interleaved topologies or several 2L-VSC modules connected in parallel can be considered a viable solution, despite the higher costs.

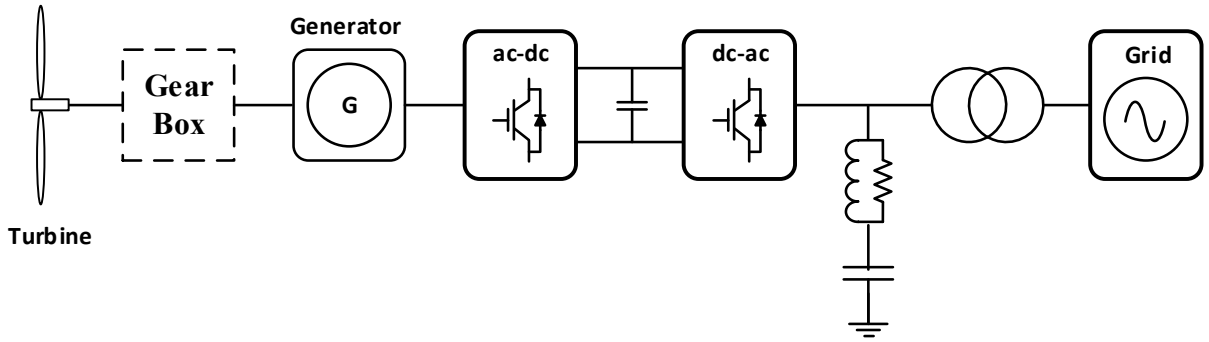

Figure 3.4. Variable speed wind turbines with a full-scale power converter.

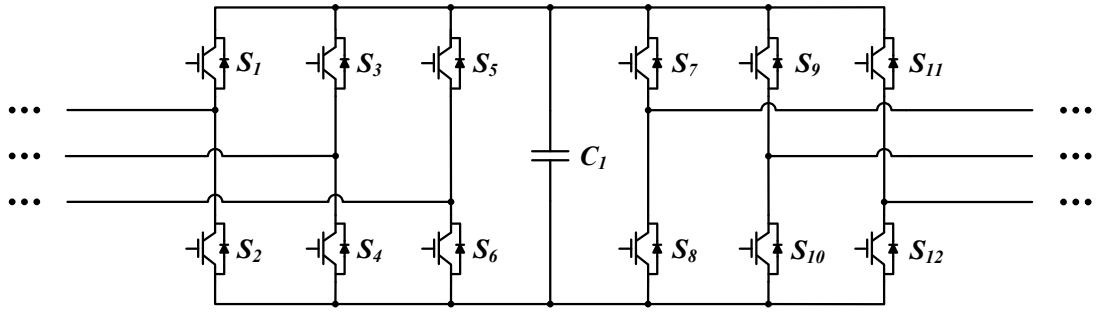

Figure 3.5. Two-level voltage source converters (2L-VSC) in back-to-back operation.

Above 3 MW, the number of power converters used starts to be considered hampering, thus increasing the cost, size, weight, and complexity of the power electronics system. However, despite the fact that the topologies employed in medium voltage (MV) are considered more suitable from an economic and energy efficiency point of view, there is still some reluctance to use them on a regular basis. This situation is justified by the fact that the availability of MV generators is very low, which contributes to an also lower scientific knowledge of MV wind turbines. Notwithstanding, some MV power converter topologies are considered: 3-level neutral point clamped VSC, 3-level and 4-level flying capacitor VSC, 3-level and 4-level diode-clamped VSC, VSC series switches, and current source converter [45].

3.1.2 Offshore Wind Turbines

Since onshore RES are normally installed in large urban centers, its connection to the power grid is considered very reliable, affordable, and flawless. However, in offshore RES-based

power production systems, due to their diversified locations, it is important to consider the transmission of power to onshore. This process is carried out underwater and two main possibilities are highlighted, high voltage alternating current (HVAC) and the high voltage direct current (HVDC).

HVAC transmission systems were the first to be adopted regarding the appearance of the first offshore wind farms. Since these production power plants were located nearshore, considered a well-consolidated technology, and with easy maintenance, HVAC was seen as a viable solution. HVAC technology has also a low cost of implementation, in short-distance transmission systems presents fewer losses and does not require the use of power converters. However, when the transmission distance increases, the losses will also increase. Moreover, HVAC underwater cables present a capacitive effect that worsens when the cable size, voltage, and power increase. For this reason, the use of HVAC for distances superior to 90 km and for large power plants can be compromised. A transmission system based on HVAC technology employs an offshore transformer (which in some instances may be dispensable, e.g., if the distance to the cost is relatively short), an onshore transformer for coupling to the power grid, HVAC underwater cables with cross-linked polyethylene (XLPE), and reactive power compensation equipment [46]–[48].

In this sense, HVDC technology allows mitigating the above-mentioned limitations of HVAC, highlighting the power transmission for large distances [49]. Thus, some alternatives regarding the converter technology can be adopted, in which line commuted converters (LCC) and voltage source converters (VSC) are becoming increasingly prevalent. The differences between these converter technologies are presented in Table 3.1 [50].

Table 3.1-Comparison between HVDC LCC and HVDC VSC.

	HVDC LCC	**HVDC VSC**
Semiconductors	Thyristor (semi-controlled)	IGBT, SiC, GaN (fully-controlled)
Power Control	Active	Active/Reactive
AC Filters	Yes	No
Minimum Short-Circuit Ratio	> 2	0
Black Start Capability	No	Yes

As observed in Table 3.1, HVDC LCC technology is based on thyristor semiconductors. This system has several advantages: (i) The transmission distance is not limited by the losses; (ii) It is possible to transmit high power at the same voltage when compared with HVAC systems; (iii) Allows an asynchronous connection; (iv) dc cables have longer lifetime; (v) possibility of controlling the flow and amplitude of the transmitted power. On the other hand, power semiconductors' switching generates harmonics, which leads to the need of including filters to mitigate this problem. Additionally, when a general collapse of the system occurs, LCC does not actively contribute to the replacement of the service (only operates when two ac ends are under voltage) and its implementation costs are higher when in comparison with HVAC systems. The implementation of HVDC LCC implies the use of converters, transformers, ac and dc filters, and dc underwater cables [50].

In turn, HVDC VSC is a more recent technology, emerging as a consequence of the evolution of power electronics systems. The development of fully-controllable semiconductors (IGBT, SiC, GaN) has triggered new opportunities for transmission in HVDC. In this way, this

technology, when compared to HVDC LCC, has a VSC in its genesis. These semiconductors can withstand higher voltages and powers, as well as controlling the system in a more efficient way, however, the switching frequency is limited. Thus, system losses, as well as harmonics and the number and size of filters are reduced. However, it is a more complex system compared to the other technologies above-mentioned [51], [52].

The control of HVDC VSC allows its operation in the four quadrants of the P-Q plane and has black start capability. In turn, fully-controlled semiconductors are more expensive devices than thyristors, the use of pulse-width modulation (PWM) control technique increases losses, and, comparing to HVDC LCC, lower power values are transmitted for the same distance. For the implementation of HVDC VSC are used power converters, transformers, ac and dc filters, and dc underwater cables [50], [51].

The configuration of HVDC transmission systems can assume different topologies, thus considering symmetric monopolar, asymmetric monopolar, bipolar, and multi-terminal architectures [53]. Symmetric monopolar systems, as observed in Figure 3.6, are the simplest configuration, in which two cables are used without including the ground reference.

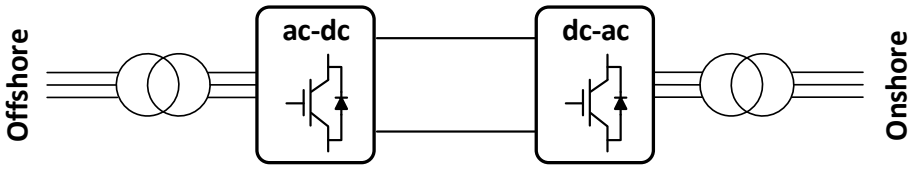

Figure 3.6. HVDC transmission system with Symmetric Monopolar configuration.

On the other hand, asymmetric monopolar structures may present two different types of configurations, metallic return or return via ground, as Figure 3.7, correspondingly demonstrate. In the case of a metallic return, two conductor cables are, once again, considered, being the return cable referenced to the ground, whereas return via ground, as the name suggests, establishes the return via ground through electrodes installed at both ends of the transmission system (only one conductor cable is used). These architectures are frequently used in areas where the resistivity of the earth is very high or if the return by water presents restrictions due to the existence of metal structures in the vicinity of the electrodes.

As with asymmetric monopolar structures, the bipolar configuration may also present two options for its implementation, shown in Figure 3.8. This configuration consists of two conductive cables with opposite polarities, being the neutral points (defined by the junction of the converters) connected to the ground, as shown in Figure 3.8 (a), or connected to each other by means of a metal cable, as shown in Figure 3.8 (b). The main advantage of this configuration, compared to monopolar, is the fact that in case of failure from one of the conductor cables, the system continues to operate, assuming the monopolar configuration. On the other hand, the implementation of this configuration has a higher cost.

(a)

(b)

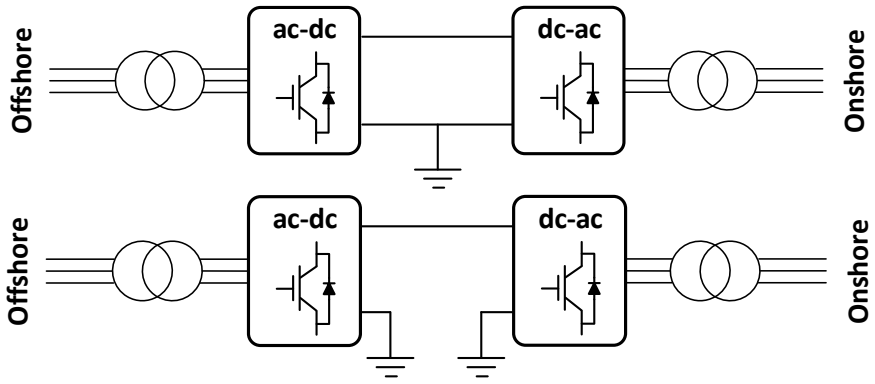

Figure 3.7. HVDC transmission system with asymmetric monopolar: (a) Configuration with metallic return referenced to the ground; (b) Configuration with return via ground.

(a)

(b)

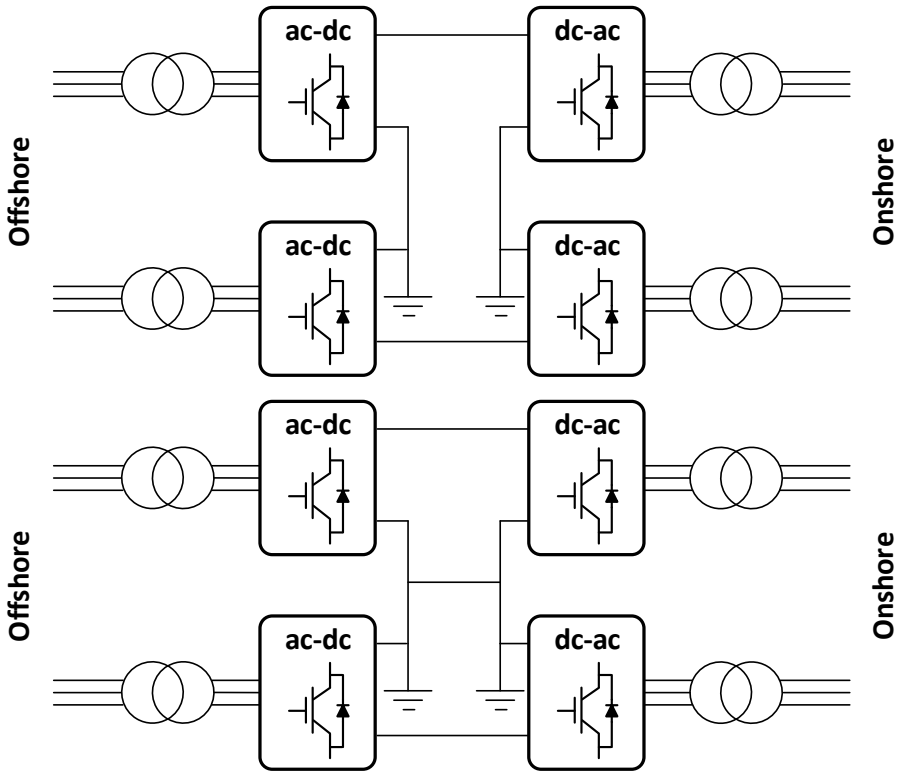

Figure 3.8. HVDC transmission system with Bipolar configuration: (a) Return by ground; (b) Metallic return.

Lastly, the multi-terminal configuration can be composed of any of the configurations above-mentioned. In Figure 3.9, it is shown an example of a 3-terminal configuration based on the symmetric monopolar configuration.

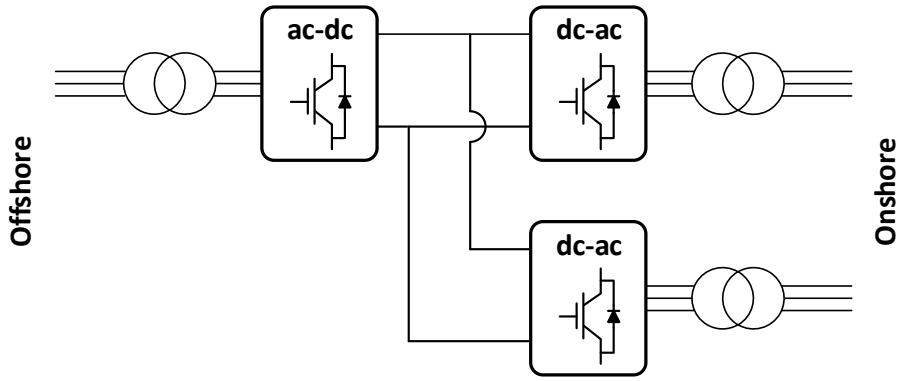

Figure 3.9. HVDC transmission system with multi-terminal configuration based on symmetric monopolar.

3.2 Solar PV Systems

As mentioned in item 2 of this book chapter, the dc power generated by a solar PV system, considering the application case, can be directly injected into the power grid or, accordingly to the smart grid concept, used to charge the ESS of a self-consumption unit or an EV, supply smart home/smart industries electrical appliances, etc. Therefore, for any of these scenarios to be considered viable, it is essential to use power electronics converters to interface the solar PV modules, enabling the extraction of their maximum power at any time of the day, as well as controlling the voltage and current values at its terminals.

3.2.1 Solar PV System Operating Principle

To maximize the efficiency of a solar PV panel, it is crucial to understand its operating principle and response to determining conditionings. In this sense, Figure 3.10 presents the equivalent electrical scheme of a single solar PV cell, contemplating the inclusion of the equivalents R_s, representative of the ohmic resistance of the semiconductor material, and R_{sh}, corresponding to electrical connection losses. Ideally, R_s would assume a value of 0 and R_{sh} would have an infinite value.

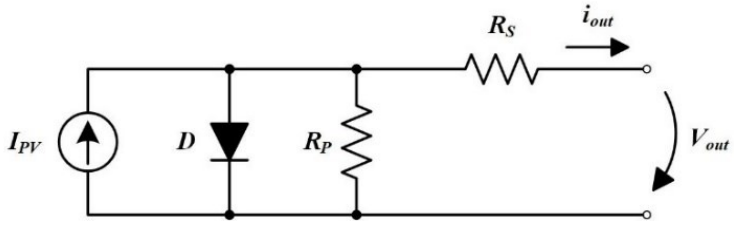

Figure 3.10. Equivalent electrical scheme of a single solar PV cell.

To trace the characteristic curves of a panel (P-V and I-V), it is essential to analyze the equivalent model of the solar PV system and obtain its output current and voltage equations. Thus, in equation (3.1), it is presented an expression for the output current of a solar PV cell ($i_{out,cell}$), considered the result of subtracting the current that flows through the diode D (i_D) and the shunt current (i_{Rsh}) to the current generated by the incident solar radiance ($i_{pv,cell}$) [54], [55].

$$i_{out,cell} = i_{pv,cell} - i_D - i_{Rsh} \tag{3.1}$$

The equivalent expressions for i_D and i_{Rsh} consider the addition of new parameters to the system. Thus, it is possible to obtain a reliable and very specific equation for $i_{out,cell}$ (3.3), in which $i_{sat,cell}$ represents the diode saturation, v_t is the thermal voltage of the cell and a is the diode ideality factor (a=1.1). Moreover, considering equation (3.2), it also should be noted that q is the elementary charge of an electron (q=1.6E10^{-19} C), k is the Boltzmann constant (k=1.38E10^{-}23 J/K), and T indicates the P-N junction working temperature in Kelvin.

$$v_t = \frac{k\,T}{q} \tag{3.2}$$

$$i_{out,cell} = i_{pv,cell} - i_{sat,cell}\left(e^{\frac{v + R_S\, i_{out,cell}}{v_t\, a}} - 1\right) - \frac{v + R_s\, i_{out,cell}}{R_{sh}} \tag{3.3}$$

However, it should also be noted that, as expected, the current generated by a solar PV panel ($i_{out,pv}$), presented in equation (3.4), is dependent on the number of cells connected in parallel (n_p) and in series (n_s), thus obtaining:

$$i_{out,pv} = n_p\, i_{pv,cell} - n_p\left(e^{\frac{\frac{v}{n_s} + \frac{R_s}{n_p} i_{out,cell}}{v_t\, a}} - 1\right) - \frac{v\,\frac{n_p}{n_s} + R_s\, i_{out,cell}}{R_{sh}} \tag{3.4}$$

Posteriorly, it is possible to trace the solar PV panel I-V (Figure 3.11(a)) and P-V (Figure 3.11(b)) curves, highlighting 3 points: I_{sc}, V_{oc}, and MPP, where:

- I_{sc} (0, I_{sc}) – Short circuit current: Maximum current extracted from a solar PV panel at the moment that its output voltage is null and the positive and negative terminals are short-circuited.

- V_{oc} (V_{oc}, 0) – Open circuit voltage: Maximum voltage at the terminals of a solar PV panel, correspondent to the moment that the latter it is not producing power (night).
- MPP (V_{MP}, I_{MP}) – Maximum power point: The moment that the power extracted from the solar PV panel assumes its maximum value.

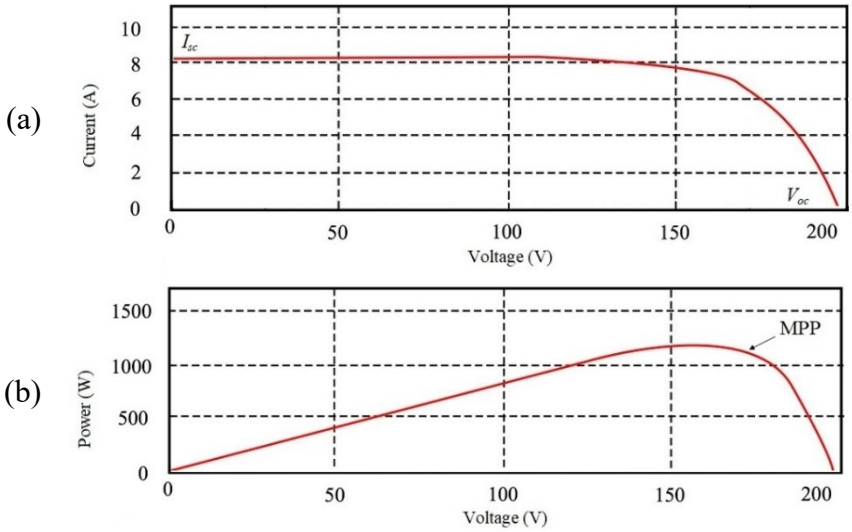

Figure 3.11. Characteristic curves of the solar PV: (a) I-V curve; (b) P-V curve.

3.2.2 Solar PV System's Efficiency Constraints

Considering the influence of certain parameters, P-V and I-V curves vary throughout the day, thus observing a constant oscillation of MPP [56]. The more intense the solar radiance, the greater the efficiency and the values of power produced (more photons will collide with the surface of each module). This situation is confirmed by the analysis of Figure 3.12, in which the influence of solar radiance on the P-V and I-V curves of a given solar PV panel is verified.

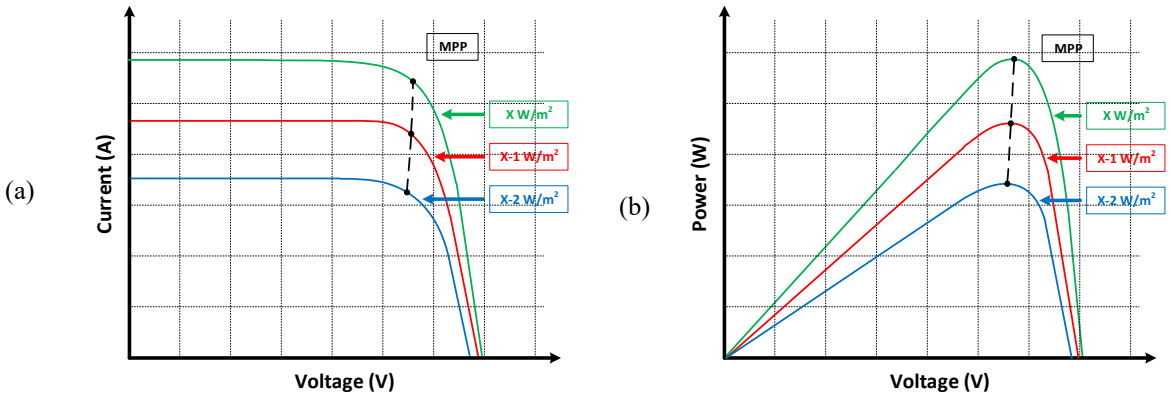

Figure 3.12. Solar radiance influence on the solar PV curves: (a) I-V curve; (b) P-V curve.

With the solar radiance increase, the greater I_{sc} and the power produced by a solar PV module (for the same voltage value), which justifies the constant oscillation of the MPP position. However, only a parcel of the radiance is absorbed by the cells, the rest being reflected or diffused. The value of incident radiance can also be affected by shading. Notwithstanding, even if the shadow effect only affects a section of the panel, the current produced by it will necessarily be lower since some of the module's cells are connected in series. In turn, the shadows can be of multiple nature, e.g., clouds or the presence of trees and buildings in the vicinity of the solar installation. Thus, the influence of this effect is observed in Figure 3.13 which shows a drastic change in the profile of the PV and I-V curves of a given solar PV panel.

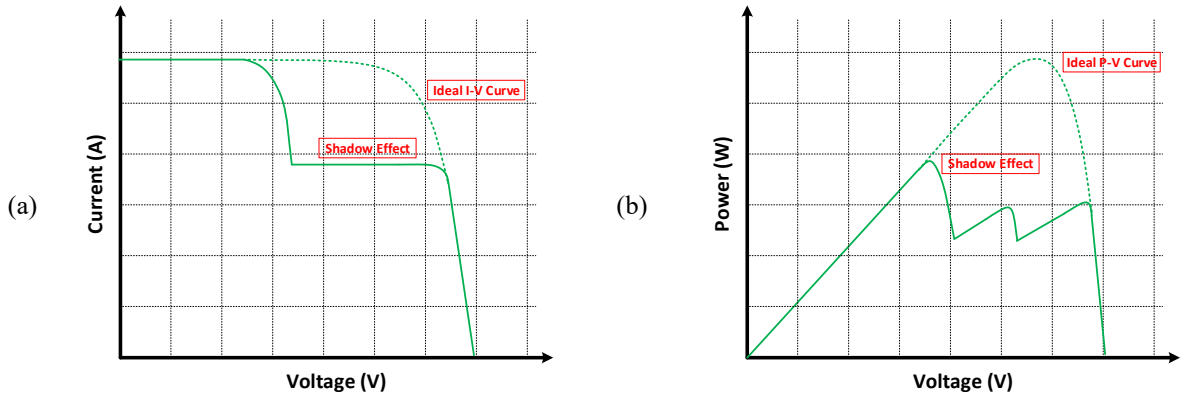

Figure 3.13. Shadow effect influence on the solar PV curves: (a) I-V curve; (b) P-V curve.

If the extracted power is higher with the increase in solar radiance, the same is not verified with the increase in ambient temperature, i.e., the higher the temperature, the lower the efficiency and power produced [57]. As mentioned, a large part of the solar radiance is not absorbed by the cells, which contributes to a lower panel efficiency and to the temperature rise. In this point of view, V_{oc} will be the main variable affected, in a dual way to the effect caused by solar radiance, where a substantial change in I_{sc} is verified. Once again, by observing Figure 3.14, it is possible to prove such statements, in which the effect of temperature on P-V (Figure 3.14(a)) and I-V (Figure 3.14(b)) curves of a given solar PV panel is verified.

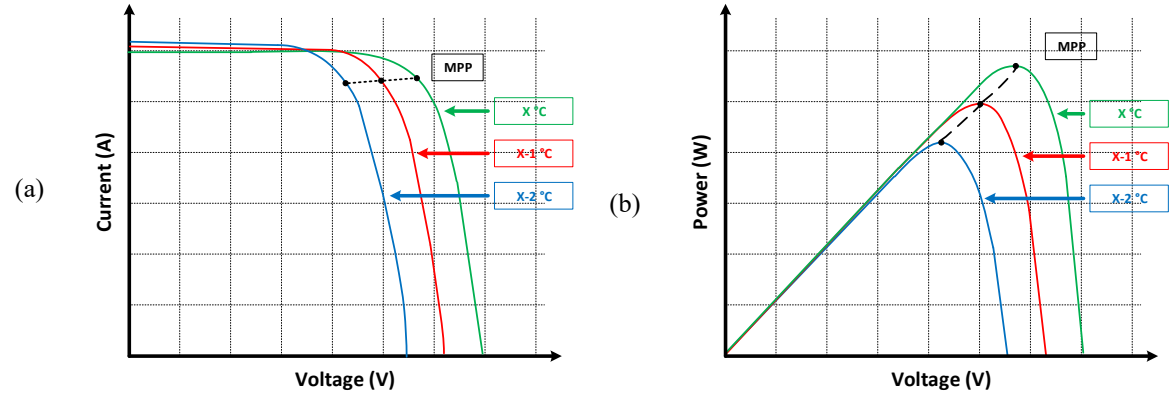

Figure 3.14. Temperature influence on the solar PV curves: (a) I-V curve; (b) P-V curve.

Another parameter that influences the efficiency and the power produced by a solar PV panel is its maintenance, considering aspects such as dirt and the accumulation of fungi/bacteria, as well as possible cracks, corrosion, or even the discoloration of its surface. Regular maintenance is essential to extend the lifetime of the modules. However, in cases of greater carelessness, they may even present a condition of non-return, not covering its acquisition cost.

3.2.3 MPPT Control Algorithms

As expected, there are several conditions and parameters that influence the ideal operation of a solar PV system, highlighting, among others, ambient temperature and incident solar radiance. Thus, as with wind power and hydropower, a maximum power point tracking (MPPT) control algorithm is used to constantly "look" for the panel's MPP, corresponding to the knee of the above presented P-V curve. Despite the high number of MPPT control algorithms, due to its ease of implementation, robustness, and capability of providing greater efficiency, MPPT Perturb & Observed (P&O) is normally applied [58]. Notwithstanding, other power converters and control algorithms may be adopted to regulate the voltage and/or current (e.g., constant voltage, fuzzy logic, artificial neural networks, incremental conductance, etc.) [59]–[62].

In the case of the P&O algorithm, the solar PV panel voltage and current are constantly verified ($v[k]$ and $i[k]$), being the latter increased or decreased with a fixed step value (*inc*) towards the MPP. The process is repeated cyclically until the point is reached. Since MPPT P&O is based on an iterative process, the search for the MPP occurs several times throughout the day. This fact constitutes a small disadvantage in sudden climatic change situations (e.g., clouds) since there will be a continuous oscillation around the MPP. For this same reason, the power losses will be slightly higher and dependent on the step value applied: the greater its value, the faster the response to sudden climatic changes, but greater the oscillation and consequent losses. Therefore, the ideal step value must be determined with computer simulations and/or experimentally. In this regard, the flowchart of the MPPT P&O control algorithm is presented in Figure 3.15.

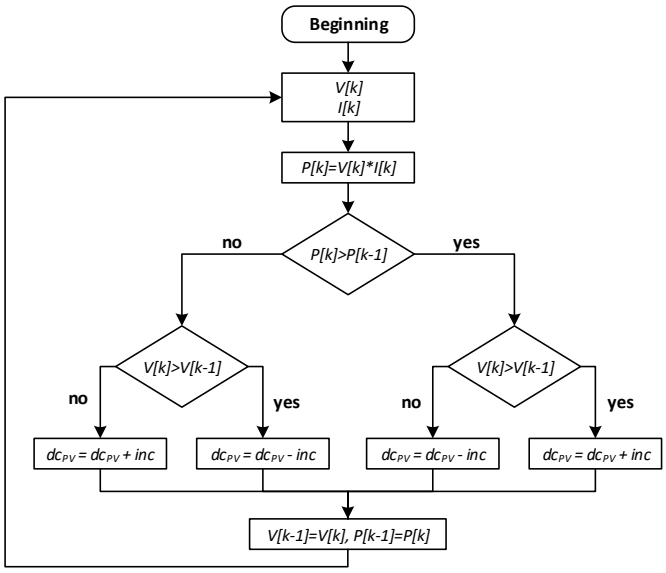

Figure 3.15. Perturb & Observe MPPT Algorithm

To mitigate the MPPT P&O control algorithm drawbacks, namely the inability to compare the array terminal voltage with the actual MPP voltage, an incremental conductance algorithm is commonly considered. Its basic concept lies in the analysis of the slope of the P-V curves, i.e., differentiating the power with respect to the voltage. At the MPP, the slope is null ($dP/dV = 0$), increases on its left side ($dP/dV > 0$), and decreases on its right ($dP/dV < 0$). At the MPP point, the following expression is obtained:

$$\frac{dP}{dV} = 0 \Leftrightarrow \frac{dI}{dV} + \frac{I}{V} \Leftrightarrow -\frac{I}{V} = \frac{dI}{dV} \tag{3.5}$$

When the MPP is reached, the PV array's instantaneous conductance (I/V) is equal to the incremental conductance (dI/dV), although with opposite values. In turn, at a different point from the MPP, it must be verified if the operating voltage is above or below its value, i.e., if the slope of the P-V curve is positive or negative. Depending on the scenario, the array voltage reference is adjusted by decreasing or increasing the previous voltage value with a fixed step value (*inc*). Since incremental conductance is an iterative control algorithm, the voltage ($V[k]$) and current ($I[k]$) values are updated in each cycle, as it is possible to observe in the flowchart of Figure 3.16.

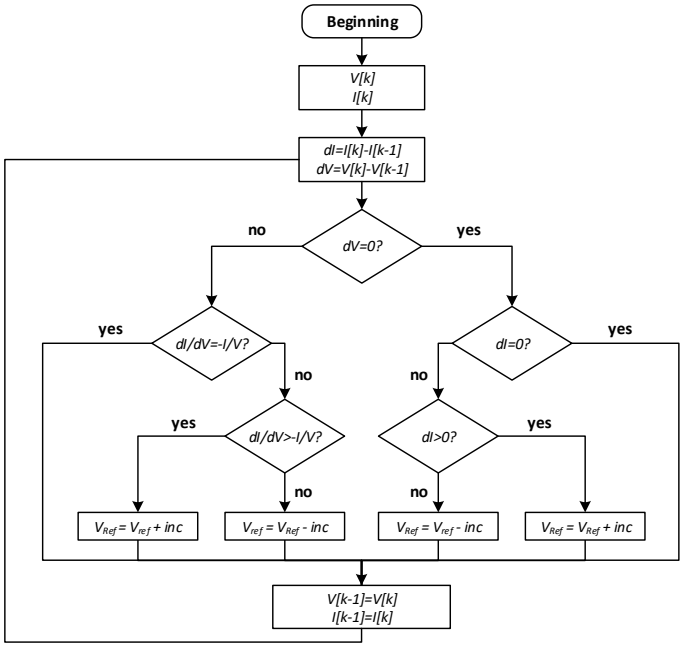

Figure 3.16. Incremental Conductance MPPT Algorithm

3.2.4 Solar PV Modules Configurations

Since the panel efficiency varies in accordance with the aforementioned conditions, new power electronics solutions must be studied and implemented, as is the case of control algorithms and power converter topologies. Moreover, to achieve certain current and voltage values, solar PV modules can be associated in series and/or parallel, thus constituting a panel. Therefore, its efficiency is affected in accordance with the connection scheme of the modules and with the architecture of the power electronics systems adopted.

As shown in Figure 3.17(a), to maximize the efficiency of a solar PV panel, each module can be equipped with a dedicated dc-ac power converter, commonly denominated by a microinverter [63]. With the adoption of this configuration, only the efficiency of a given module would be affected, e.g., by the action of a shadow or due to dirt, maintaining the overall efficiency of the solar panel at higher values. This situation is also verified in the series microinverter configuration (Figure 3.17(b)), in which the efficiency of each module is obtained independently [64]. However, the interface with each solar PV module is now achieved with a dc-dc power converter, allowing to connect all modules in series. In other words, the nominal power is higher compared to the parallel microinverter configuration, but the lower efficiency values of a specific module do not influence the rest of the solar PV panel. Lastly, to interface loads, electrical appliances, ESS, etc., a single-phase inverter is commonly used.

(a)

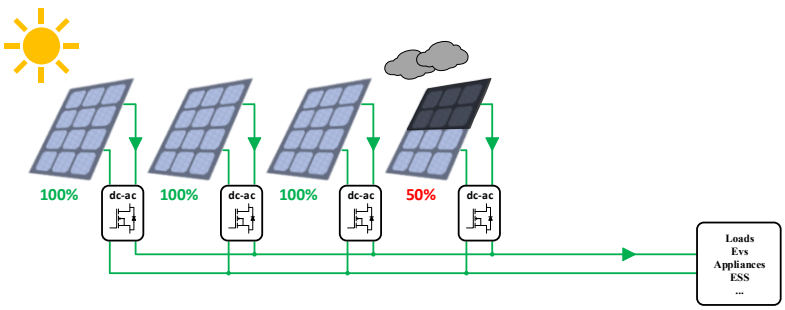

(b)

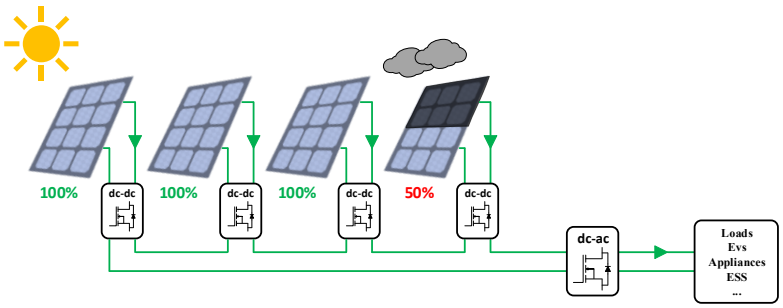

Figure 3.17. Microinverter configurations for solar PV system: (a) Parallel; (b) Series.

The use of a dedicated power converter for each module represents higher implementation costs, the reason why, in most solar PV systems, only one single-phase inverter is used for each solar PV panel (string), as Figure 3.18 shows. As mentioned, in a string inverter configuration, all the modules are connected in series and only one single phase inverter is used per string, which may compromise its efficiency [65].

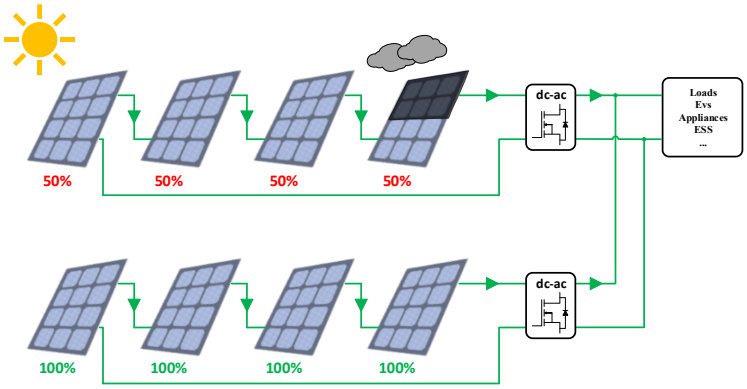

Figure 3.18. String inverter configuration for solar PV systems.

However, contrary to string inverter configuration, central inverter units only consider the use of one single-phase inverter for the entire solar PV system [66]. This configuration, presented in Figure 3.19, as its name suggests, is a centralized architecture in which the single-phase inverter deals with much higher nominal power values [67]. Notwithstanding, the main difference between these configurations relies on its flexibility, i.e., if a certain module fails, the entire operation of the solar PV system is compromised in a central inverter configuration, only one string is affected in a string inverter configuration and only the module in failure is compromised in series microinverter and parallel microinverter configurations. Independently of the chosen configuration, there will always exist a tradeoff between the cost (number of power converters used) and the efficiency of the solar PV system.

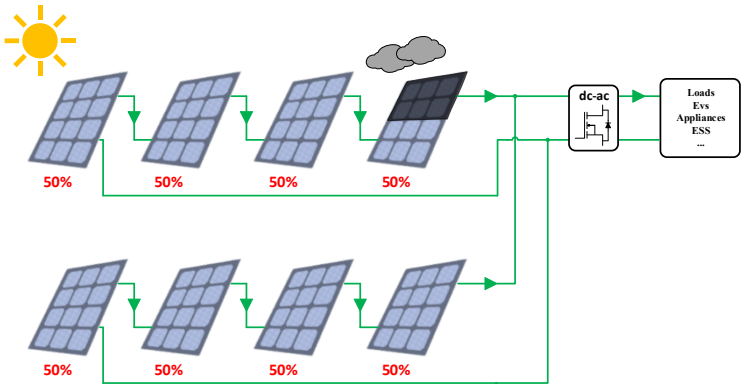

Figure 3.19. Central inverter configuration for solar PV systems.

In a multistring inverter configuration, and just as for the string inverter, the efficiency of each panel is independent of the solar PV system as a whole, which is not the case, e.g., for the central inverter configuration. However, and as can be seen in Figure 3.20, the interface with each of the strings is performed using a dc-dc power converter, the output of which is connected to a single dc-link. The use of an intermediary dc-dc conversion stage, besides facilitating the optimal operation of the panels (MPP), provides voltage decoupling capability and allows the operation of the solar PV system over a wider range of voltage values. For this reason, the number of modules that constitute each string is considered more flexible. On the other hand, since this configuration is seen as a two-stage architecture, the total conversion losses are slightly higher [68], [69].

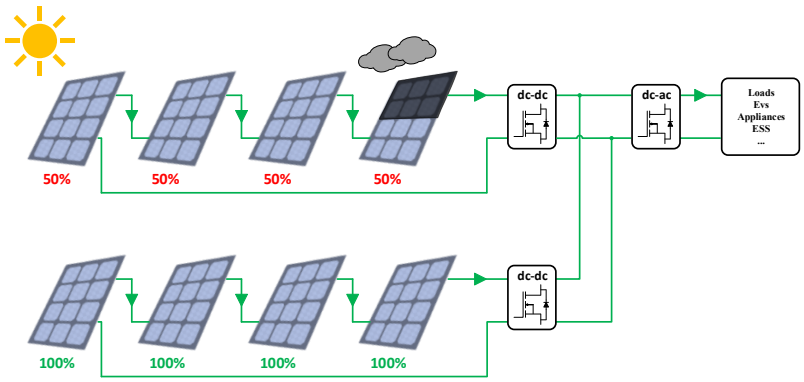

Figure 3.20. Multistring inverter configuration for solar PV systems.

3.2.5 Dc-dc Power Converter Topologies

According to the power of the solar PV system, several dc-dc converter topologies can be adopted, including isolated and non-isolated architectures. In this respect, for solar PV systems in which the voltage and current values are considered low, basic buck-type (Figure 3.21(a)) and boost-type (Figure 3.21(b)) converters are normally used.

The buck and boost topologies, presented in Figure 3.21, share the same ground point and are considered inexpensive, but, on the other hand, generate large values of electromagnetic noise. For both of them, the components that are in its genesis are a diode, a fully-controlled semiconductor, an inductor, and two capacitors, the latter responsible for attenuating the voltage ripple at the input (V_{in}) and output (V_{out}) terminals of the power converter. Depending on the application, if V_{in} is higher than the required V_{out}, a buck power converter must be adopted, employing a boost power converter if the opposite occurs, i.e., if V_{in} is lower than the required V_{out}. In this respect, the characteristic equations of the buck-type and boost-type converters are indicated, correspondingly, in equation (3.6) and equation (3.7), in which V_{out} is provided in accordance with the relation between V_{in} and the duty-cycle (D) of the signal applied to the semiconductor S_1.

$$V_{out} = V_{in}\, D \tag{3.6}$$

$$V_{out} = V_{in}\, \frac{1}{1 - D} \tag{3.7}$$

On the other hand, when V_{out} is intended to assume a specific value, the aforementioned buck and boost power converters can also be connected in series, which, in other words, is named a cascade power electronics converter. In this sense, the ratio between V_{out} and V_{in} is a multiple of the number of interlinked converters. Thus, in Figure 3.22 is shown an example of the boost-type topology in a cascade association.

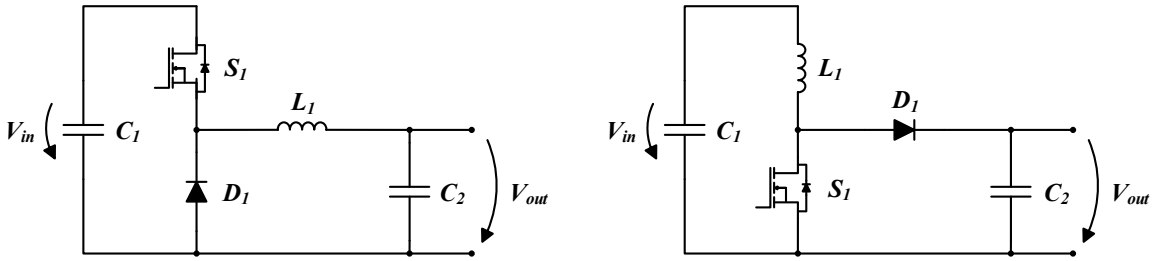

Figure 3.21. Dc-dc power converter topologies: (a) Buck-type; (b) Boost-type.

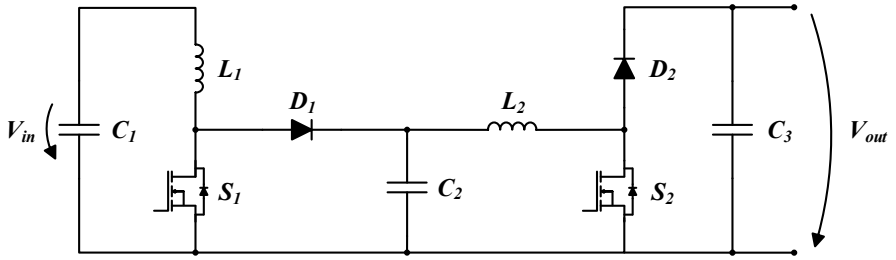

Figure 3.22. Boost-type topology in cascade.

The functionalities of the buck and boost power converters can be combined in a buck-boost type converter, in which V_{out}, depending on the value applied to D, presents a higher or lower value than V_{in}. This topology, as for the buck-type and boost-type converters, is also constituted by a diode, a fully-controlled semiconductor, an inductor, and two capacitors, as it is possible to observe in Figure 3.23(a). Thus, if D is greater than 50%, V_{in} is equal to V_{out}. Below this value, the converter operates in buck mode, entering boost mode when D is greater than 0.5. This situation is verified in equation (3.8), thus concluding that the conversion scale of this topology is more limited than the aforementioned architectures. That is, in buck-type and boost-type topologies, the value of D could vary freely from 0% to 100%, however, in this case, each of the operating modes only has a range of 50% for the variation of D.

$$V_{out} = V_{in} \frac{D}{1 - D} \tag{3.8}$$

For very specific solar PV applications, where is intended to, e.g., reduce switching losses, voltage ripple, or current oscillations, power converter topologies such as SEPIC (Figure 3.23(b)), Zeta (Figure 3.23(c)), and Cuk (Figure 3.23(d)) may be employed. These, despite providing determined and, as mentioned, specific operating characteristics to the system, also present a large number of drawbacks when in comparison with the buck-boost architecture, as is the case of higher costs, elevated implementation difficulty, and inefficient and low conversion rate. However, studies related to these topologies are frequently found in the literature, among others, presenting their advantages and drawbacks, energy efficiency analyses [70].

In medium/high power electronics systems, it is essential to adopt new converter topologies that are capable of meeting the current energy needs. Thus, multilevel converters, as mentioned, are seen as a viable solution for medium/high power systems, since a large number of semiconductors are normally used. This characteristic allows dividing the voltage through them, thus reducing losses and extending their lifetime. However, increasing power levels will also increase the associated costs. Notwithstanding, by applying specific control algorithms, it is possible to obtain more voltage levels at the output of the converter, which, consequently, is reflected in better results in terms of power quality.

Comparing to conventional topologies, multilevel converters allow to increase the power of the system without changing the maximum current value and to improve power quality standards, e.g., reducing harmonic distortion and voltage transients. With these measures, the dynamic response of the converter is faster and there is the possibility of increasing the switching frequency of the semiconductors, which, among other aspects, reduces the size of converter passive elements (inductors, transformers, and capacitors). On the other hand, since the number of semiconductors is higher, the complexity of the control algorithms will also be according to the number of levels that can be obtained in the output of the conversion stage.

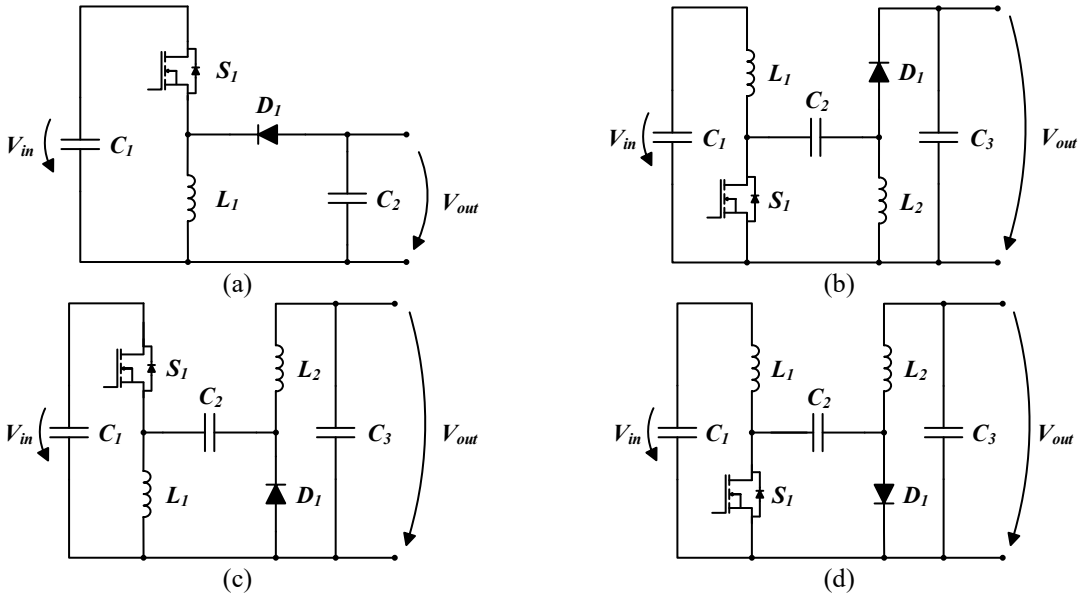

Figure 3.23. Dc-dc power converter topologies: (a) Buck-boost; (b) SEPIC; (c) Zeta; (d) Cuk.

The possibility of obtaining more voltage levels in the output of the converter makes multilevel topologies considered ideal for the implementation of bipolar grids, increasingly disseminated in the literature and seen as one of the possible structures to be adopted in active buildings in the context of smart grids. As observed by the analysis of Figure 3.24, compared to traditional unipolar grids, based on a two-wire configuration (one voltage level), bipolar structures present an additional wire (three wires, two voltage levels) and lower complexity. Since bipolar grids present greater flexibility, its implementation aims to respond to the constant evolution of the types of loads and electrical appliances connected to the power grid, characterized by, among other aspects, presenting different voltage levels. Thus, with the inclusion of a new voltage level, the efficiency of the conversion stages is higher, as well as the controllability in conditions of a line fault. However, it is essential to control and mitigate possible voltage unbalances and obtain balanced currents from the point of view of the power grid.

As mentioned, the use of multilevel topologies increases the global efficiency of solar PV systems. In the case of a 3-level symmetric boost converter, the voltage across the inductor, active semiconductors, and diodes is reduced to half. When compared to a 2-level topology, for a determined ripple current, the inductance can also be reduced to half, thus decreasing the size, cost, and weight of the inductor. In this specific topology, the third voltage level is created by splitting the input dc-link. Many other multilevel topologies can be considered, highlighting, e.g., the 3-level flying capacitor boost due to its higher efficiency [71].

In addition to multilevel topologies, also interleaved converters are commonly adopted in medium/high power scenarios. Such architectures provide greater energy efficiency since the ripple frequency is higher, as much as the number of arms (n) of the converter connected in parallel. Thus, the stress in the power semiconductors and the conduction losses are also

reduced since the nominal current is divided by *n* arms. Bearing in mind that the number of semiconductors is higher, it is expected that the implementation difficulty will also be so. However, since the ripple frequency is *n* times higher, the size and weight of the passive components of a dc-dc converter are lower. In the literature, several interleaved topologies to interface solar PV systems are found [70], [72]. Thus, examples of boost-type interleaved, and multilevel power converters are presented in (Figure 3.25(a)) and (Figure 3.25(b)).

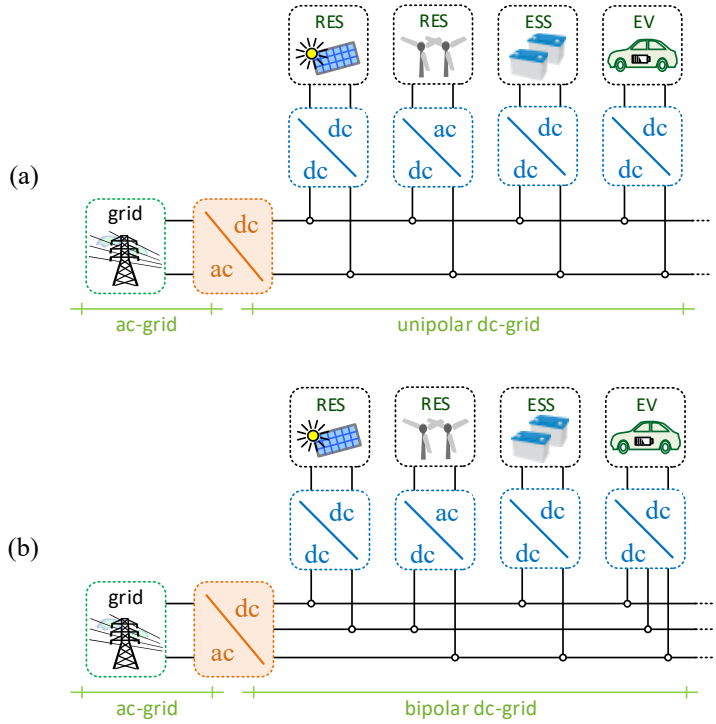

Figure 3.24. Power grid architecture comparison: (a) Traditional unipolar grids, based on a two-wire configuration; (b) Bipolar grids, based on a three-wire configuration.

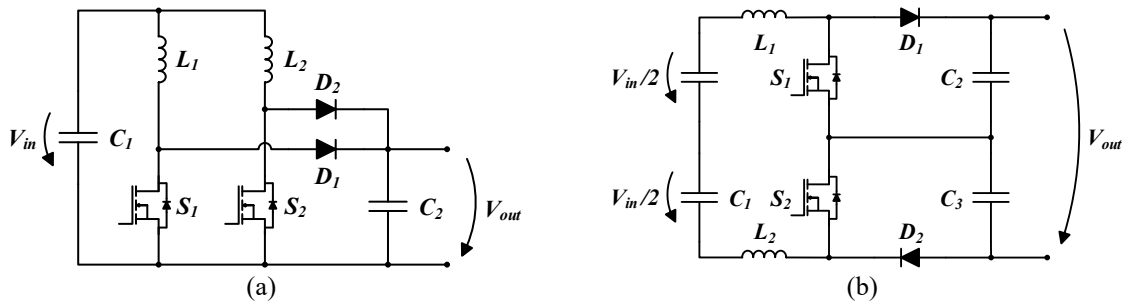

Figure 3.25. Boost Topologies: (a) Interleaved boost; (b) 3-level symmetric boost.

On the other hand, in certain power electronics systems, dc-dc unidirectional isolated topologies must be employed in order to provide greater safety and, among other features, regulate the voltage values according to the transformer transformation ratio. In the literature, are commonly introduced, among others, the topologies full bridge transformer isolated buck converter (Figure 3.26(a)), half bridge transformer isolated buck converter (Figure 3.26(b)), forward converter (Figure 3.26(c)), flyback converter (Figure 3.26(d)), push-pull converter (Figure 3.26(e)), and phase shift full bridge converters (Figure 3.26(f)) [70].

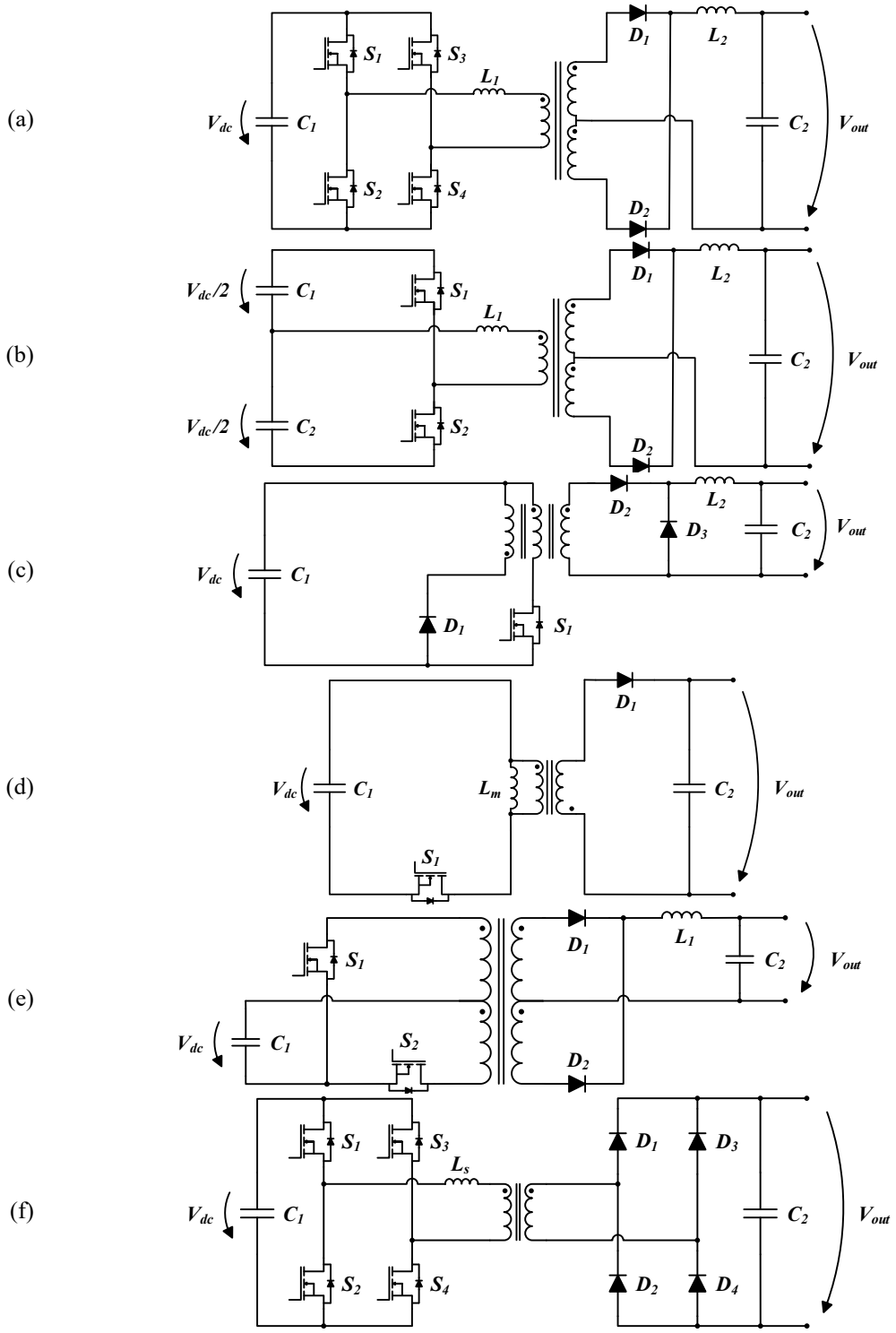

Figure 3.26. dc-dc unidirectional isolated topologies: (a) Full bridge transformer isolated buck converter; (b) Half bridge transformer isolated buck converter; (c) Forward converter; (d) Flyback converter; (e) Push-pull converter; (f) Phase shift full bridge converters.

3.2.6 Dc-ac Power Converter Topologies

As previously mentioned, regardless of the solar PV system configuration (microinverter, central inverter, etc.), it is essential to properly accomplish the interface between the modules (or panels) and the power grid. If, on the one hand, dc-dc power converters are used to regulate the power generated by the modules (MPPT), solar inverters, in turn, assume a central role in

energy management and efficiency. According to the application scenario, the chosen configuration, and the nominal power values of the system, several solar inverter topologies are depicted in the literature. For each one of them, different parameters must be considered, as is the case of galvanic isolation, leakage currents, voltage fluctuations, and grounding issues, however, the cost, volume, and weight are also addressed.

In Figure 3.29, the main transformerless inverter topologies for a string configuration are presented, being normally employed due to their reduced cost and higher efficiency. The most common inverter topologies are conventional half-bridge (Figure 3.29(a)) and full-bridge (H4, Figure 3.29(b)), highly efficient and reliable inverter concept (HERIC, Figure 3.29(c)), H5 (Figure 3.29(d)), and H6 architectures (Figure 3.29(e)-Figure 3.29(g)), the latter presenting modified versions. Conventional full-bridge is a well-known and reliable topology, however, improved versions are also commonly used to increase efficiency. In comparison with half-bridge topology, the full-bridge semiconductors do not have to support higher voltage values, the dc-link is not divided, and three voltage values can be obtained in V_{out} by employing a unipolar control. In solar PV systems, since half-bridge topologies demand the double of the input voltage, either a large number of panels connected in series or boost dc-dc conversion stage need to be considered.

In transformerless architectures, common-mode (CM) leakage currents are considered a major drawback, leading to serious safety and radiance interference issues. To mitigate leakage currents, CM voltage (V_{CM}) must be kept constant, which can be assured by applying a sinusoidal pulse width modulation (SPWM). Bipolar SPWM, although presenting good leakage current characteristics, provokes, on the other hand, higher switching losses and current ripple, as shown in Figure 3.27. Unipolar SPWM (Figure 3.28), in turn, has a smaller inductor current ripple, however V_{CM} varies at switching frequency [69]. Several solutions were studied to kept V_{CM} constant and reduce leakage currents, which lead to the research and development of new converter topologies, as is the case of HERIC [73], H5 [74], and H6-type [75].

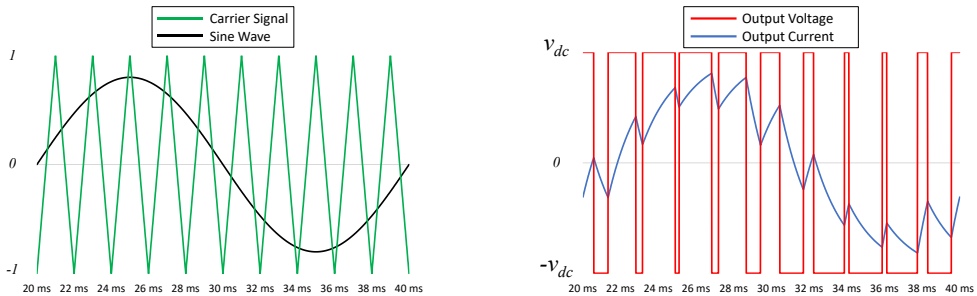

(a) (b)

Figure 3.27. Bipolar SPWM: (a) Carrier and sine wave signals; (b) Output voltage and current.

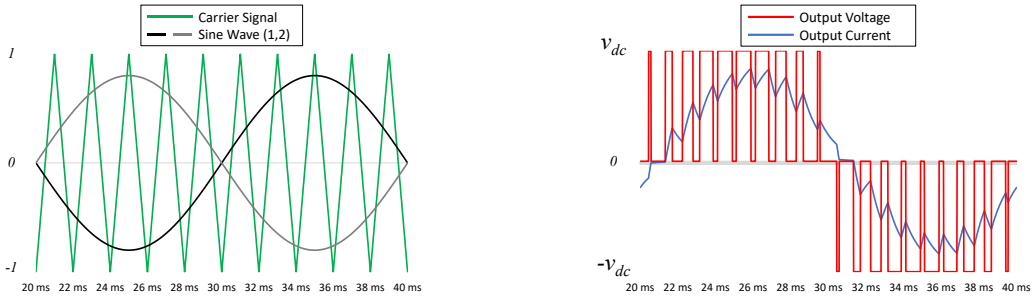

(a) (b)

Figure 3.28. Unipolar SPWM: (a) Carrier and sine wave signals; (b) Output voltage and current.

H5-type topology, as the name suggests, presents an additional semiconductor that allows the disconnection of the PV string from the power grid when the output voltage is at zero level, thus eliminating the leakage current path. HERIC topology, as it is possible to observe in Figure 3.29(c), presents an ac bypass leg, obtained by connecting back-to-back semiconductors in parallel with the bridge. The semiconductors S5 and S6 are responsible to isolate the solar PV string from the power grid and prevent reactive power exchange between the filter's inductors and dc-link capacitors during zero voltage state [73]. Thus, and as with H5-type topology, the leakage current path is eliminated, which increases the efficiency overall efficiency.

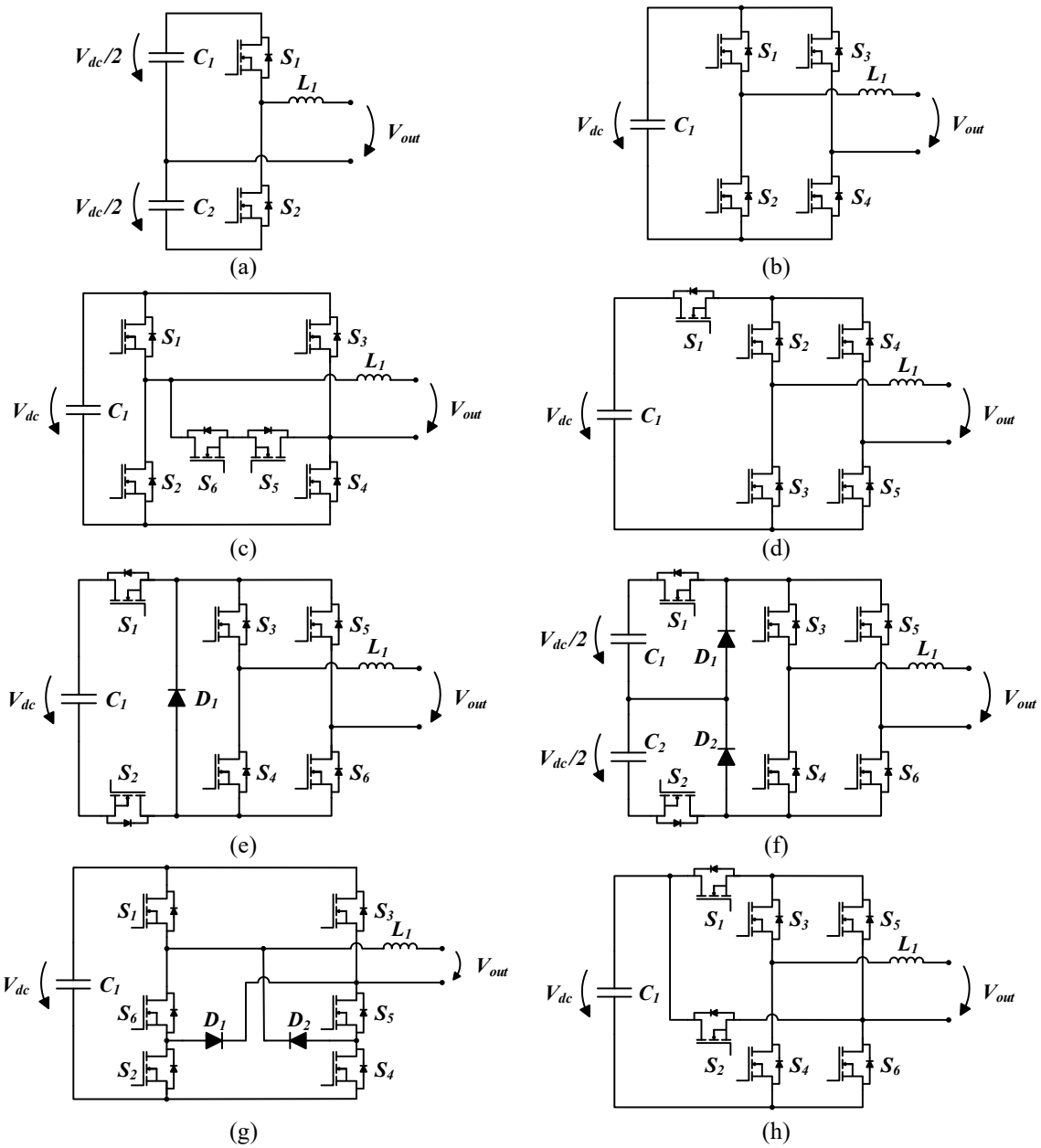

Figure 3.29. String PV inverter topologies: (a) Half-Bridge; (b) H-Bridge (H4); (c) HERIC; (d) H5; (e) Conventional H6D1; (f) Conventional H6D2; (g) Modified H6D2 (1); (h) Modified H6D2 (2).

HERIC inverters, in comparison with H5 and H6-type topologies, have lower conduction losses, but, on the other hand, present the least efficient operation regarding V_{CM}. H6-type topologies, in turn, presents the best V_{CM}. characteristics. The conventional structure of the H6-type inverter includes an additional semiconductor connected to the negative point of the

dc-link, however two main different architectures are considered: H6D1 (Figure 3.29(e)) and H6D2 (Figure 3.29(f) and Figure 3.29(g)). Other structures may also be considered, as Figure 3.29(h) shows [69]. With the inclusion of a new semiconductor, it is formed a new current path that allows to reduce conduction losses and, accordingly to the diode arrangements, leakage currents can be eliminated.

To increase the solar PV inverters' efficiency, several aspects may be considered, as is the case of the adoption of suitable control algorithms, new semiconductor technologies (SiC, GaN, etc.), and the use of multilevel or interleaved topologies. Comparing to two-level inverters, although the higher cost, weight, and volume, multilevel topologies present higher efficiency due to lower switching losses, reduce dv/dt stress, are ideal to improve power quality standards (e.g., low harmonic distortion) and dynamic stability, the electromagnetic interference (EMI) is more reduced, and are almost non-limited in term of levels number.

Cascaded multilevel inverters consist of the connection in series of n dc-ac converters, being the output voltage of this stage, the sum of the voltage generated by each module. Thus, $2n+1$ voltage levels are generated, while, for k voltage levels, $2(k-1)$ semiconductors are used. In this regard, a 5-level cascade converter based on a full-bridge topology is presented in Figure 3.30(a), in which V_{out} assumes the values of $+2V_{CC}$, $+V_{CC}$, 0, $-V_{CC}$, and $-2V_{CC}$. Notwithstanding, as mentioned, many other levels can be obtained with the stacking of other inverter modules.

Contrary to cascade multilevel inverters, flying capacitor topologies presented a divided dc-link, meaning that the maximum voltage level of V_{out} is limited to $+V_{CC}/2$. Thus, Figure 3.30(b) shows a 5-level flying capacitor inverter constituted by 8 semiconductors, as the abovementioned cascade topology. In comparison with other multilevel topologies, flying capacitor is able to regulate the voltages levels through redundant states, thus proving the versatility of this architecture [76].

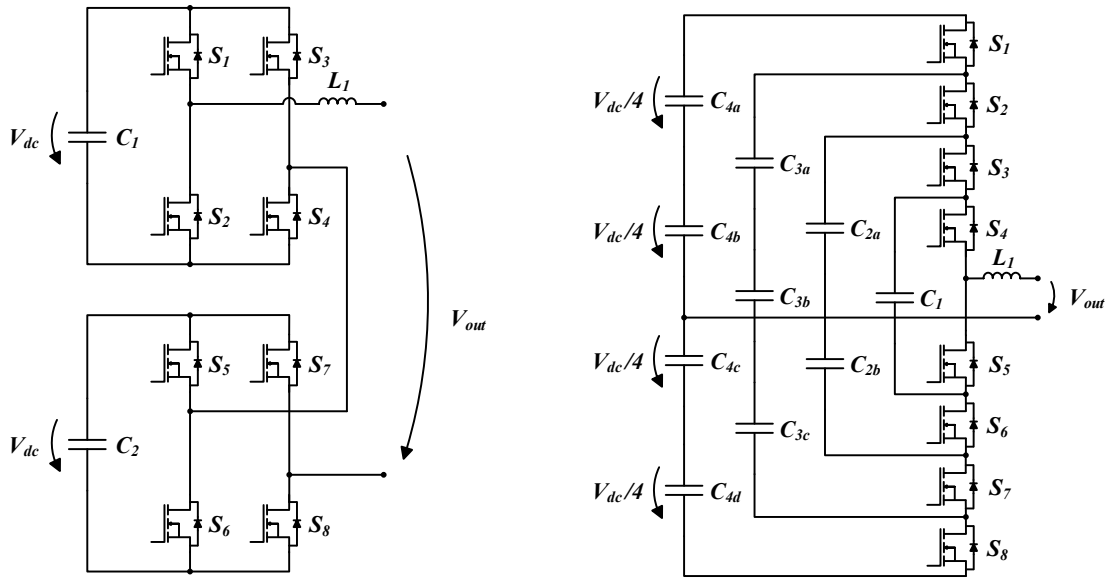

Figure 3.30. Multilevel PV inverter topologies: (a) 5-level cascade H4; (b) 5-level flying capacitor.

As abovementioned, designing and implementing a transformerless inverter requires particular attention with regard to its efficiency and leakage currents. As with HERIC, H5, and H6-type topologies, also neutral point clamped (NPC) architectures are considered a suitable solution to mitigate leakage currents by keeping V_{CM} constant. Thus, diode neutral point clamped (DNPC, Figure 3.31(a)) and active neutral point clamped (ANPC, Figure 3.31(b)) multilevel converters are also one of the main inverter topologies employed in solar PV systems

with string, multistring, or central inverter configuration. Depending on the voltage levels that can be obtained in $V_{out,}$ the number of diodes and active semiconductors varies, e.g., a 3-level DNPC is constituted by 4 active semiconductors and 2 diodes, whereas a 5 level DNPC has 8 active semiconductors and 6 diodes. Since each device of the DNPC topology presents different losses, ANPC architecture is able to mitigate such a situation with the use of suitable control algorithms [77], [78]. Notwithstanding, for both cases (and also for other multilevel topologies, e.g., flying capacitor and cascade-type inverters), SPWM and space vector modulation are widely used, however, the greater the number of V_{out} voltage levels, the greater the complexity of the control.

Comparing to DNPC, ANPC and diode stacked NPC (DSNPC, Figure 3.31(c)) have more zero switching states that can be used to double the apparent switching frequency. The existence of a single zero switching state (as in DNPC) has a direct consequence on the total loss distribution among each device, thus decreasing its efficiency [79]. However, both for ANPC and DSNPC, there are active semiconductors that switch on the entire cycle, which limits the output power and the maximum switching frequency. To overcome these drawbacks, an ASNPC (Figure 3.31(d)) was proposed in [80]. This topology is derived from the DSNPC, having two additional active semiconductors connected antiparallel with the clamp diodes. The main advantage of the ASNPC is its capability of reducing in half the average switching frequency on the entire cycle for all the devices and making the apparent switching frequency twice the switching frequency. Such characteristics make ASNPC a very attractive solution for medium-voltage and high-power applications.

To limit ground leakage current, positive negative NPC (PN-NPC, Figure 3.31(e)) and negative positive NPC (PN-NPC, Figure 3.31(f)) are also commonly considered. Besides de mitigation of $V_{CM,}$ PN-NPC topology also allows the use of lower voltage semiconductors, thus increasing the overall efficiency of the inverter [81].

Figure 3.31(g) presents a 5-level full-bridge NPC (5L-FB-NPC) topology, considered one of the main novelties for solar PV inverters. Compared to traditional full-bridge, as the name suggests, it can synthesize an output voltage waveform with 5 voltage levels, thus reducing V_{CM}, harmonic distortion, electromagnetic interferences, and output current ripple [69]. Lastly, in Figure 3.31(h) is shown a T-type NPC, where the inner active semiconductors (S_5-S_8) connect the ac output terminal to the neutral dc input. Compared to a 3-L DNPC inverter, T-type NPC is less complex and presents lower total semiconductor losses, however its use is considered more appropriate for low/medium frequencies [82].

Regardless of the chosen inverter topology, the output current waveform is always dependent on the adopted control technique. Among the literature, several techniques are depicted, from those that are considered simpler (hysteresis current control and periodic sampling) to those that present the greatest implementation difficulty, but, at the same time, that provide sinusoidal waveforms with lower THD%, and with unitary power factor. Among the latter, predictive or proportional-integral (PI) current control techniques are commonly used with SPWM modulation.

A PI control technique with SPWM modulation is considered linear, thus allowing to obtain a fixed switching frequency and facilitate the design of the passive filters. However, as the main drawback, this control technique is not as efficient in the face of sudden changes in the reference signal. Besides, when it is intended to synthesize different current references, the proportional and integral values must be adjusted. On the other hand, predictive control with SPWM modulation is based on the electric model of the system, in which it is calculated the

necessary voltage (v_{ref}) to obtain the desired output current. Although the predictive control is also linear (thus presenting a fixed switching frequency), the response to sudden reference changes is faster (lower THD%) and there is no need to readjust any parameter.

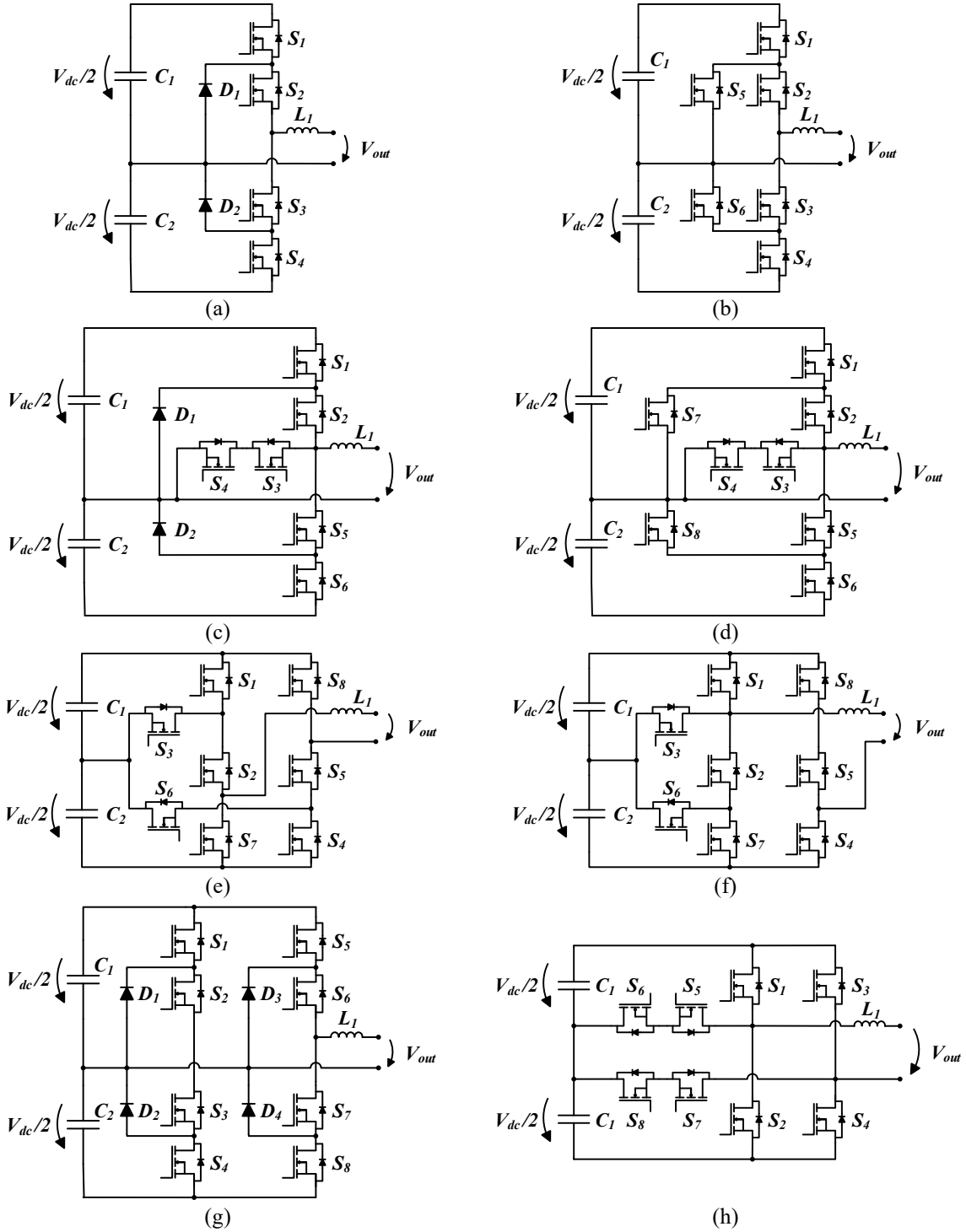

Figure 3.31. NPC inverter topologies: (a) 3L-DNPC; (b) 3L-ANPC; (c) 3L-DSNPC; (d) 3L-ASNPC; (e) PN-NPC; (f) NP-NPC; (g) 5L-FB-DNPC; (h) T-type NPC.

The above presented dc-ac topologies are considered suitable for string, multistring and central inverter configurations. However, in most of the microinverter architectures, it is essential to, in only one power converter unit, constantly extract the maximum available power

(MPPT), step-up and invert a low dc voltage produced by a solar module (20 V - 30 V) to a relatively high ac voltage (230 V RMS), and allow current and voltage control at the output of the stage. Since a microinverter is dedicated to a single module, its design must be compact and the use of bulky low-frequency transformers is not required, thus increasing the overall efficiency, flexibility and modularity. Compared to conventional string inverters, microinverter configurations easily allow the detection of failures and are considered more suitable for domestic PV systems due to its redundancy, cost, and power density (the rated power is between 100 W and 400 W).

The conversion of low voltage generated by the solar PV module to a determined ac current must be carried out with the maximum efficiency, which can be accomplished with the use of single-stage and two-stage topologies [83]. Thus, microinverters are classified as: high-frequency dc-link in single-stage topology, high-frequency two-stage topology, and single-stage topology with two-stage configuration. Despite the drawbacks regarding leakage currents, non-isolated topologies are emerging in the literature due to their higher efficiency.

Comparing to two-stage topologies, single-stage architectures are less expensive, present greater efficiency, and are more compact. As mentioned, a single-stage inverter combines the step-up and inverter capabilities in one power stage, which can also lead to the use of a lower number of components (semiconductors, etc.). On the other hand, large electrolytic capacitors are required to limit the voltage ripple at the terminals of the solar PV module. Such a scenario is also verified in two-stage topologies, in which electrolytic capacitors are used between the dc-dc and the dc-ac stages. These components are expensive and have reduced lifetime due to their exposure to high temperatures, being necessary to converge to other solutions, e.g., the use of ceramic and film capacitors, interleaved topologies, SiC and GaN-based semiconductors, etc. It is imposed that the microinverter lifetime must be longer than that of the solar PV module.

Thus, in Figure 3.32, some non-isolated power converter topologies for microinverter configurations are presented. Among the literature, several topologies are depicted, most of them based on conventional boost and buck-boost architectures. Figure 3.32(a) shows a double-boost microinverter topology, firstly proposed in [84] by Fang et al. The use of coupled inductors (L_1-L_4) in this single-state architecture allows: (i) to generate a sinusoidal current waveform that depends on the duty-cycle value and also on the turn ratio of the coupled inductors; (ii) reduce the output voltage and input current ripple; (iii) reduce the volume and weight of the microinverter in high-frequency application. Moreover, the use of two-coupled inductor double-boost converters connected in parallel aims to allow the operation of the inverter is quad quadrants, which cannot be accomplished with a boost converter. As with the abovementioned non-isolated topologies, a SPWM can be implemented to generate a sinusoidal waveform. The modulation of each converter has a mismatch of 180°, maximizing the voltage excursion of V_{out}.

Buck-boost-based architectures are also commonly used in single-stage inverter applications. In this regard, Figure 3.32(b) presents a two-inductor buck-boost single-stage inverter. Comparing to other buck-boost topologies, this architecture presents reduced switching losses and components, however, constraints regarding even-order harmonics on the

dc-side, low voltage gain, and low efficiency arise. Another variation of this topology is proposed in [85], in which the main objective is to obtain higher gains, thus replacing the two inductors by switched inductors. The previous gain is improved by $\sqrt{2}$, however, the cost and number of components used is higher.

In Figure 3.32(c), a two-stage microinverter based on a buck-boost topology is presented, also commonly known as Aalborg inverter [86]. As is the case for the vast majority of solar PV inverter architectures, this topology was conceived to mitigate leakage currents, however the number of active switches increases and there are limitations regarding dc input voltage range, voltage conversion ratio, and lifetime of the decoupling electrolytic capacitor. In turn, only one power stage works at high-frequency, while the output stage (current source inverter, H-bridge) works at line frequency, thus generating an output sinusoidal wave with low harmonic distortion. Since and inductor is "saved" due to the arrangement of the boost and buck stages, the conduction losses are reduced, and higher efficiency values are achieved. In addition to the above presented non-isolated buck-boost topologies, an extensive review of single-stage buck-boost inverters is presented in [87].

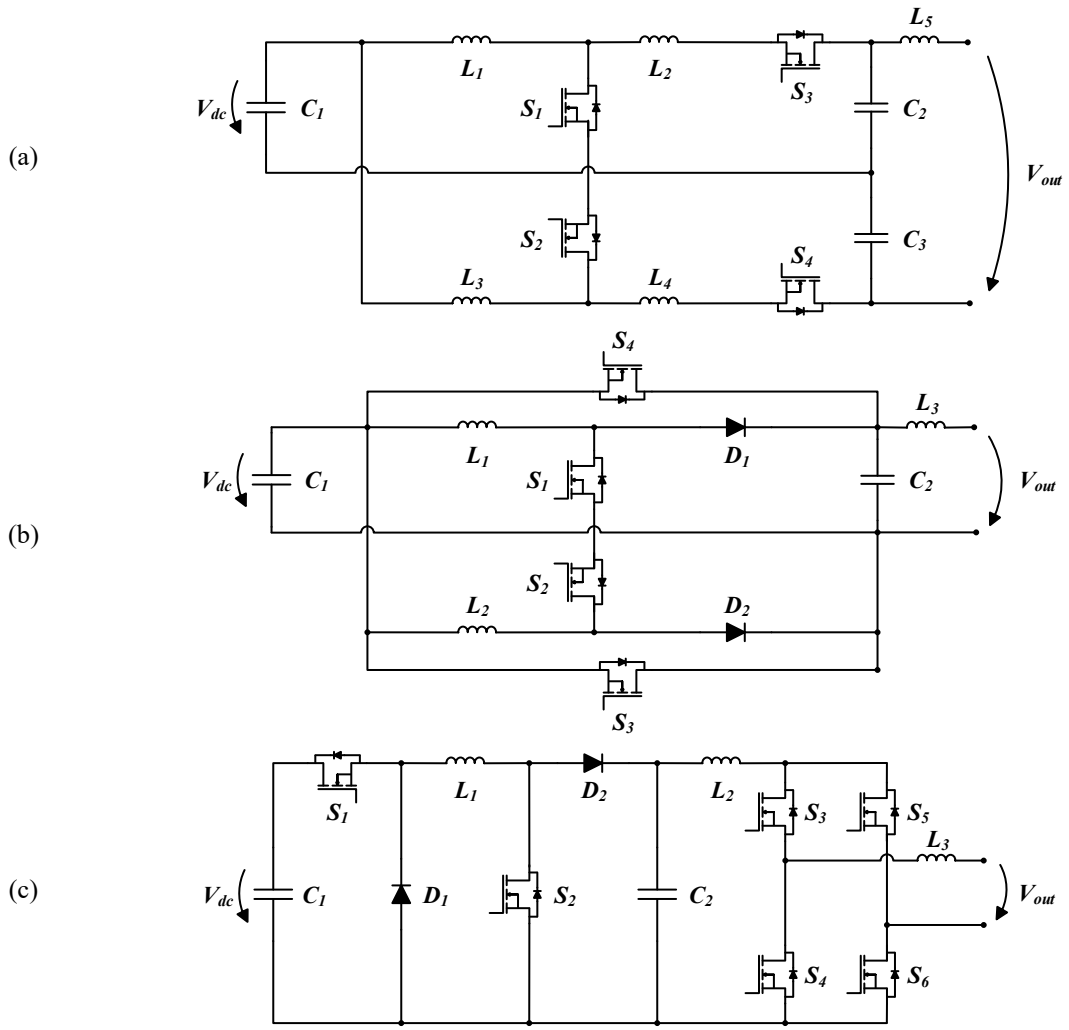

Figure 3.32. Non-isolated power converter topologies for microinverter configurations: (a) Two-inductor single-stage boost; (b) Single-stage buck-boost; (c) Two-Stage Buck-boost.

As abovementioned, transformerless topologies present higher efficiency, improved compactness, and reduced cost, size, and weight compared to isolated topologies. However, issues regarding CM leakage currents are a major drawback, causing several disturbances related to safety, electromagnetic interference, grounding issues, increased THD%f, etc. Thus, to keep V_{CM} constant and, consequently, reduce leakage currents, new and innovative transformerless topologies are depicted in the literature. Notwithstanding, the existence of physical isolation between the solar PV system and the power grid (high-frequency transformer) provides higher reliability to the system, mitigating CM disturbances, assuring galvanic isolation, and allowing higher boosting values in accordance with the transformation ratio of the high-frequency transformer. As observed in Figure 3.33, the complexity of isolated inverters is increased since the number of semiconductors, capacitors, etc., is higher, thus partially justifying its lower efficiency comparing to transformerless architectures.

Figure 3.33 (a) shows a current-fed push-pull converter with a full-bridge inverter. Due to its high-boosting capability, the step-up ratio of the high-frequency transformer can be minimized, however, conduction losses and stress over the semiconductors are increased [88]. As for the current-fed push-pull converter, flyback topologies are also commonly applied in microinverter configurations due to its higher step-up capability and robustness. The conventional flyback converter followed by a full bridge inverter is presented in Figure 3.33(b). As is it possible to observe, a high-frequency transformer is used to provide galvanic isolation and increase the step-up ratio. Given the duty-cycle value (D) applied to S_1 and the transformer ratio ($N=N_1/N_2$), the output voltage of the conventional flyback converter (V_{C2}) is defined as follows:

$$V_{C2} = \frac{N_2 D}{N_1(1-D)} V_{dc} \tag{3.9}$$

Nonetheless, an interleaved flyback converter followed by a full-bridge inverter is presented in Figure 3.33(c). Compared to the conventional flyback topology, interleaved architectures have more active switches and can operate in three modes: discontinuous conduction mode (DCM), boundary conduction mode (BCM), and continuous conduction mode (CCM). Several topologies are commonly used for DCM operation, in which switching, conduction, and copper losses are more reduced when the rated power increases. When the opposite happens, i.e., the rated power decreases, the core losses are minimized. However, in DCM control, the converter operates as a current source, thus causing higher current stress on the primary side of the high-frequency transformer and consequently decreasing its efficiency. To overcome these drawbacks, interleaved topologies with CCM control (Figure 3.*33*(c)) are considered robust, highly-efficient, and present low voltage stress, and almost null electromagnetic interference. Moreover, the converter operation is not affected by load changes due to the existence of two large magnetizing inductances (L_{M1} and L_{M2}). BCM mode occurs during the transition between DCM and CCM. The operation in this mode aims to improve output power quality and power density, however switching and gate driving losses are much higher [69], [89].

A flyback inverter with center-tapped secondary winding is presented in Figure 3.33(d). This topology has a reduced cost due to the low number of components used, however, its efficiency is lower due to the need of applying an elevated turns ratio so that high-boosting capability is achieved. In turn, to improve power decoupling and global efficiency values, a

single stage innovative topology based on three-port flyback (Figure 3.33(e)) was proposed by Hu et al. in 2012 [90]. One of the main objectives of this work was to extend the lifetime of the film capacitors, considered one of the main challenges regarding microinverter configurations. As mentioned, the lifetime of the microinverter must match the lifetime of the solar PV module, i.e., approximately 25 years, which can be compromised when the electrolytic capacitors are used as a power decoupling element. Moreover, the proposed decoupling circuit is also responsible for mitigating leakage energy, which means that additional dissipative circuits are not required. Consequently, the power losses are reduced and the efficiency is increased.

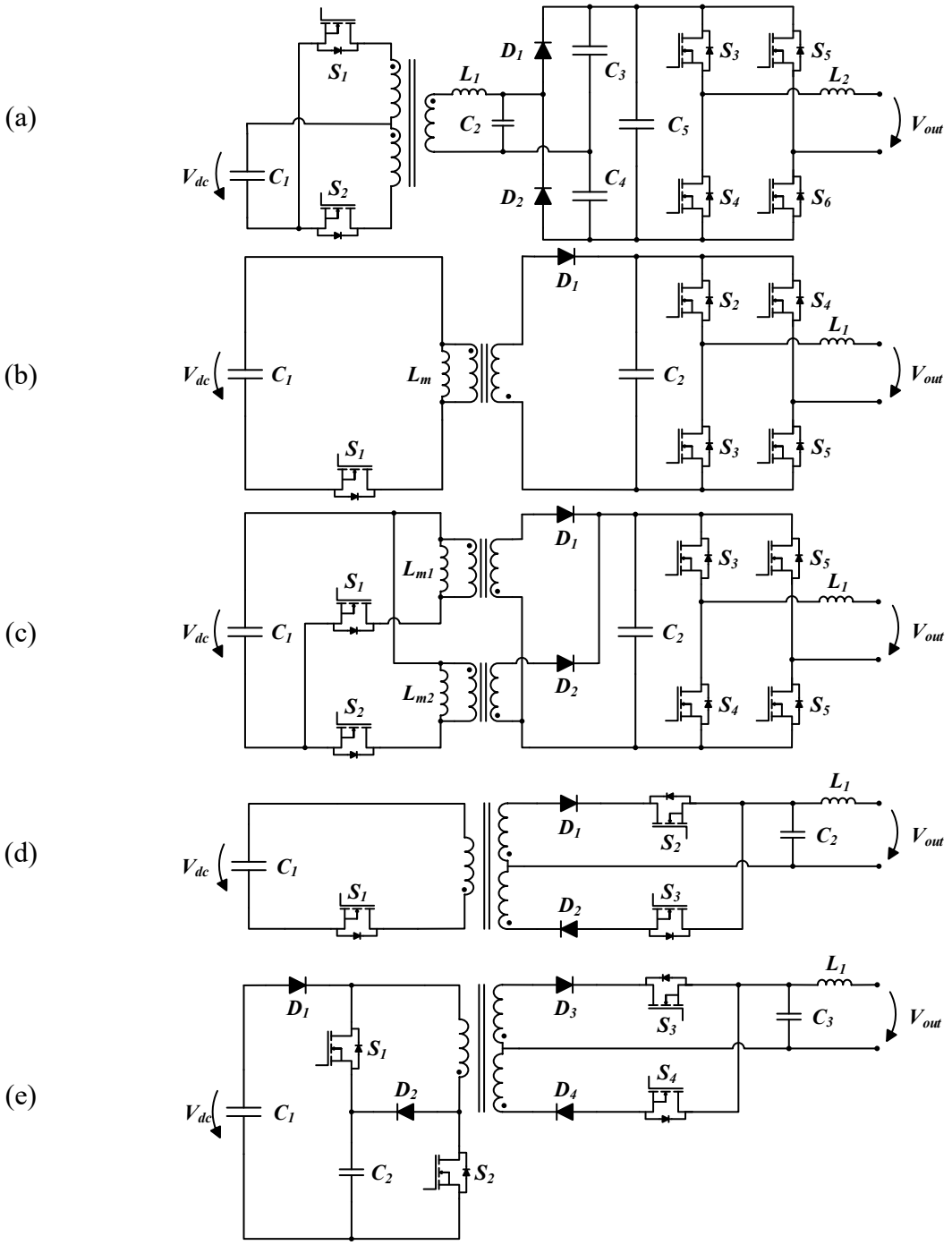

Figure 3.33. Isolated power converter topologies for microinverter configurations: (a) Current-fed push-pull inverter; (b) Conventional two-stage flyback; (c) Interleaved two-stage flyback; (d) Single-stage flyback with center-tapped secondary winding; (e) Single-stage three-port flyback.

As mentioned, Figure 3.33(a), Figure 3.33(b), and Figure 3.33(c), are considered in the literature as two-stage inverter topologies. As the name implies, the first stage is responsible for extracting the maximum available power and for increasing the voltage generated by the solar PV module, while the second stage has the inverter function. Figure 3.34(f) and Figure *3.34*(g) are also two-stage inverter topologies, in which a full-bridge inverter is once again used in the second stage of the power converter. Figure 3.34(f) presents a boost half-bridge converter, in which, as mentioned, a low input dc voltage is boosted by a high-frequency transformer and inverted, in the first stage, by a half-bridge. However, the energy stored in L_S causes high-voltage stress on the components, the reason why an integrated voltage clamp circuit is included to discharge the energy of L_S without additional components [83]. In Figure 3.34(g), a two-stage inverse buck current-fed dual-boost inverter is shown. This topology allows to achieve a higher step-up ratio and improve the conversion efficiency, however, a large number of components is used. As mentioned in [91], high MPPT accuracy characteristics can also be achieved.

(a)

(b)

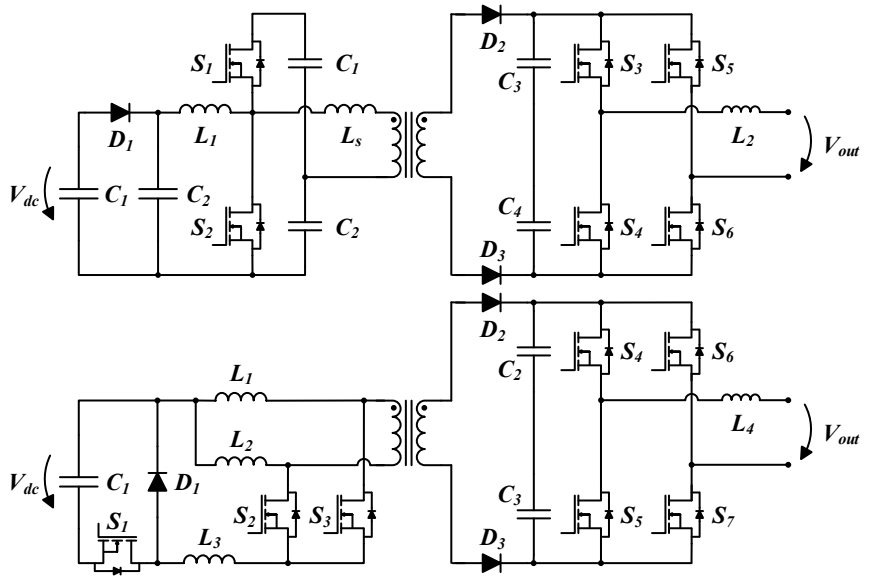

Figure 3.34. Isolated power converter topologies for microinverter configurations: (a) Two-stage boost half bridge; (b) Two-stage inverse buck current-fed dual-boost.

4 Conclusions

Due to the objective of reducing CO_2 emissions to the atmosphere, renewable energy sources (RES) are gaining special preponderance in the power grid. Recent technological developments in this area have allowed RES to become more competitive in relation to fossil fuels, also reinforced by environmental commitments established worldwide. As discussed in section 2 of this book chapter, although several types of RES are considered in this book chapter, only a few of them are commercially available, with the prospect that this situation will change in the coming years and new renewable energy generation methods will be increasingly consolidated. The interface with RES must be carried out with adequate topologies of power converters and control algorithms. In most cases, converter costs, efficiency, and complexity are the variables that influence its dissemination and use, however, in the context of smart grids, the choice of such topologies is also influenced by the integration of more and more technologies in the power grid (e.g., renewables, energy storage systems and electric vehicles). As a fundamental requirement for smart grids, for the aforementioned examples, ac-

dc and dc-dc converters with bidirectional power flow must be used, however, the RES interface is based on unidirectional ac-dc and dc-dc topologies. Depending on the values of power involved, isolated and non-isolated topologies are also considered. Thus, in section 3, dc-dc and dc-ac power converter topologies to interface RES are addressed, which constitutes an important contribution of this book chapter. Moreover, in the same section, offshore power transmission architectures are also depicted, highlighting the main features, as well as pros and cons. According to the advantages associated with offshore power production, it is expected to observe a continuous growth of offshore power production units over the next years.

Acknowledgment

This research was funded by the European Regional Development Fund (ERDF) through the Northern Regional Operational Program, grant number NORTE-01-0247-FEDER-037417 EcOffShorBe—Eco Offshore Built Environment.

References

[1] R. M. Elavarasan *et al.*, "A Comprehensive Review on Renewable Energy Development, Challenges, and Policies of Leading Indian States with an International Perspective," *IEEE Access*, vol. 8, pp. 74432–74457, 2020.

[2] O. Ogunrinde, E. Shittu, and K. K. Dhanda, "Investing in renewable energy: Reconciling regional policy with renewable energy growth," *IEEE Engineering Management Review*, vol. 46, no. 4, pp. 103–111, 2018.

[3] S. M. Hakimi and S. M. Moghaddas-Tafreshi, "Optimal planning of a smart microgrid including demand response and intermittent renewable energy resources," *IEEE Transactions on Smart Grid*, vol. 5, no. 6, pp. 2889–2900, 2014.

[4] F. Blaabjerg, Y. Yang, and K. Ma, "Power electronics - Key technology for renewable energy systems - Status and future," *2013 3rd International Conference on Electric Power and Energy Conversion Systems, EPECS 2013*, pp. 0–5, 2013.

[5] E. J. Coster, J. M. A. Myrzik, B. Kruimer, and W. L. Kling, "Integration issues of distributed generation in distribution grids," *Proceedings of the IEEE*, vol. 99, no. 1, pp. 28–39, 2011.

[6] F. Blaabjerg, Z. Chen, and S. B. Kjaer, "Power electronics as efficient interface in dispersed power generation systems," *IEEE Transactions on Power Electronics*, vol. 19, no. 5, pp. 1184–1194, 2004.

[7] J. M. Carrasco *et al.*, "Power-electronic systems for the grid integration of renewable energy sources: A survey," *IEEE Transactions on Industrial Electronics*, vol. 53, no. 4, pp. 1002–1016, 2006.

[8] M. Liserre, T. Sauter, and J. Y. Hung, "Future energy systems: Integrating renewable energy sources into the smart power grid through industrial electronics," *IEEE Ind. Electron. Mag*, vol. 4, pp. 18–37, 2010.

[9] F. Blaabjerg, R. Teodorescu, M. Liserre, and A. v. Timbus, "Overview of control and grid synchronization for distributed power generation systems," *IEEE Trans. Ind. Electron.*, vol. 53, no. 5, pp. 1398–1409, 2006.

[10] R. Teodorescu, M. Liserre, and P. Rodriguez, *Grid Converters for Photovoltaic and Wind Power Systems*. 2011.

[11] S. B. Kjaer, J. K. Pedersen, and F. Blaabjerg, "A review of single-phase grid-connected inverters for photovoltaic modules," *IEEE Trans. Ind. Appl*, vol. 41, no. 5, pp. 1292–1306, 2005.

[12] D. Meneses, F. Blaabjerg, Ó. García, and J. A. Cobos, "Review and comparison of step-up transformerless topologies for photovoltaic AC-module application," *IEEE Transactions on Power Electronics*, vol. 28, no. 6, pp. 2649–2663, 2013.

[13] F. Blaabjerg, M. Liserre, and K. Ma, "Power electronics converters for wind turbine systems," *IEEE Transactions on Industry Applications*, vol. 48, no. 2, pp. 708–719, 2012.

[14] F. Blaabjerg and K. Ma, "Future on power electronics for wind turbine systems," *IEEE Journal of Emerging and Selected Topics in Power Electronics*, vol. 1, no. 3, pp. 139–152, 2013.

[15] B. Kroposki *et al.*, "Achieving a 100% Renewable Grid: Operating Electric Power Systems with Extremely High Levels of Variable Renewable Energy," *IEEE Power and Energy Magazine*, vol. 15, no. 2, pp. 61–73, 2017.

[16] V. Monteiro, J. G. Pinto, and J. L. Afonso, "Experimental Validation of a Three-Port Integrated Topology to Interface Electric Vehicles and Renewables with the Electrical Grid," *IEEE Transactions on Industrial Informatics*, vol. 14, no. 6, pp. 2364–2374, 2018.

[17] V. Monteiro, J. Afonso, T. J. C. Sousa, and J. L. Afonso, "The Role of Off-Board EV Battery Chargers in Smart Homes and Smart Grids: Operation with Renewables and Energy Storage Systems," in *Electric Vehicles in Energy Systems*, 1st ed., SPRINGER, 2019, pp. 47–72.

[18] K. Huang, W. Xiang, L. Xu, and Y. Wang, “Hybrid AC/DC hub for integrating onshore wind power and interconnecting onshore and offshore DC networks,” *IET Renewable Power Generation*, vol. 14, no. 10, pp. 1738–1745, 2020.

[19] Y. Pipelzadeh, N. R. Chaudhuri, B. Chaudhuri, and T. C. Green, “Coordinated Control of Offshore Wind Farm and Onshore HVDC Converter for Effective Power Oscillation Damping,” *IEEE Transactions on Power Systems*, vol. 32, no. 3, pp. 1860–1872, 2017.

[20] A. Harrouz, D. Belatrache, K. Boulal, I. Colak, and K. Kayisli, “Social Acceptance of Renewable Energy dedicated to Electric Production,” *9th International Conference on Renewable Energy Research and Applications, ICRERA 2020*, pp. 283–288, 2020.

[21] D. G. de E. e Geologia, “Renováveis: Estatísticas rápidas - no 193,” 2020.

[22] N. Chattha, R. Karki, and F. Fang, “Seasonal reservoir management in hydro dominant power systems to enhance availability,” *2017 IEEE Electrical Power and Energy Conference, EPEC 2017*, vol. 2017-Octob, pp. 1–5, 2018.

[23] J. Qu, W. Shi, K. Luo, C. Feng, and J. Mou, “Day-ahead Generation Scheduling Method for New Energy and Hydro Power System,” *2018 International Conference on Power System Technology, POWERCON 2018 - Proceedings*, pp. 1899–1902, 2019.

[24] C. S. Canalejo, R. Sarrias-Mena, P. Garcia-Trivino, and L. M. F. Ramirez, “Energy management system design and economic feasibility evaluation for a hybrid wind power/pumped hydroelectric power plant,” *IEEE Lat. Am. Trans*, vol. 17, no. 10, pp. 1686–1693, 2019.

[25] A. E. Samani, N. Kayedpour, J. D. M. de Kooning, and L. Vandevelde, “Performance and Structural Load Analysis of Small and Medium Wind Turbines Operating with Active Speed Stall Control versus Pitch Control,” *2019 IEEE 2nd International Conference on Renewable Energy and Power Engineering, REPE 2019*, pp. 241–247, 2019.

[26] S. D. Ahmed, F. S. M. Al-Ismail, M. Shafiullah, F. A. Al-Sulaiman, and I. M. El-Amin, “Grid Integration Challenges of Wind Energy: A Review,” *IEEE Access*, vol. 8, pp. 10857–10878, 2020.

[27] S. F. Hui, H. F. Ho, W. W. Chan, K. W. Chan, W. C. Lo, and K. W. E. Cheng, “Floating solar cell power generation, power flow design and its connection and distribution,” *2017 7th International Conference on Power Electronics Systems and Applications - Smart Mobility, Power Transfer and Security, PESA 2017*, vol. 2018-Janua, pp. 1–4, 2018.

[28] S. E. R. I. of Singapore, “Floating Solar Market Report,” *Where Sun Meets Water*, 2019.

[29] E. Du *et al.*, “The role of concentrating solar power toward high renewable energy penetrated power systems,” *IEEE Transactions on Power Systems*, vol. 33, no. 6, pp. 6630–6641, 2018.

[30] J. Ji, V. Raoupatham, N. Sittibud, and N. Nananukul, “Biomass power generation supply chain planning,” *2017 IEEE International Conference on Smart Grid and Smart Cities, ICSGSC 2017*, pp. 115–119, 2017., and N. A. Rahim, “Technical review on biomass conversion processes into required energy form,” *CEAT 2013 - 2013 IEEE Conference on Clean Energy and Technology*, pp. 208–213, 2013.

[32] A. von Jouanne and T. K. A. Brekken, “Ocean and Geothermal Energy Systems,” *Proceedings of the IEEE*, vol. 105, no. 11, pp. 2147–2165, 2017.

[33] H. Kulasekara and V. Seynulabdeen, “A Review of Geothermal Energy for Future Power Generation,” *5th Int. Conf. Adv. Electr. Eng.*, pp. 223–228, 2019.

[34] N. Bartels, G. Bussmann, and R. Ignacy, “Geothermal Energy in the Context of the Energy Transition Process,” *2018 Int. IEEE Conf. Work. Óbuda Electr. Power Eng*, pp. 103–108, 2018.

[35] H. Polinder and M. Scuotto, “Wave energy converters and their impact on power systems,” *2005 Int. Conf. Futur. Power Syst.*, pp. 1–9, 2005.

[36] S. S. Prakash *et al.*, “Wave Energy Converter: A Review of Wave Energy Conversion Technology,” *2016 3rd Asia-Pacific World Congr. Comput. Sci. Eng. (APWC CSE)*, pp. 71–77, 2016.

[37] European Commission, “Ocean Energy Strategic Roadmap: Building Ocean Energy for Europe,” *Ocean Energy Forum*, p. 74, 2016, [Online]. Available: https://webgate.ec.europa.eu/maritimeforum/en/frontpage/1036

[38] I. Páscoa, C. Camus, and E. Eusébio, “Technical and economic assessment of energy from tidal currents,” *Renewable Energy and Power Quality Journal*, vol. 1, no. 13, pp. 101–107, 2015.

[39] A. Achilli, T. Y. Cath, and A. E. Childress, “Selection of inorganic-based draw solutions for forward osmosis applications,” *Journal of Membrane Science*, vol. 364, no. 1–2, pp. 233–241, 2010.

[40] R. Adiputra, T. Utsunomiya, J. Koto, T. Yasunaga, and Y. Ikegami, “Preliminary design of a 100 MW-net ocean thermal energy conversion (OTEC) power plant study case: Mentawai island, Indonesia,” *Journal of Marine Science and Technology (Japan)*, vol. 25, no. 1, pp. 48–68, 2020.

[41] C. C. K. Liu, “Ocean thermal energy conversion and open ocean mariculture: The prospect of Mainland-Taiwan collaborative research and development,” *Sustainable Environment Research*, vol. 28, no. 6, pp. 267–273, 2018.

[42] S. M. Masutani and P. K. Takahashi, “Ocean thermal energy conversion (OTEC),” *Encyclopedia of Ocean Sciences*, no. 4, pp. 641–647, 2019.

[43] A. Hossain, A. Azhim, A. B. Jaafar, M. N. Musa, S. A. Zaki, and D. N. Fazreen, “Ocean thermal energy conversion: The promise of a clean future,” *CEAT 2013 - 2013 IEEE Conference on Clean Energy and Technology*, pp. 23–26, 2013.

[44] F. Iov, M. Ciobotaru, D. Sera, R. Teodorescu, and F. Blaabjerg, “Power electronics and control of renewable energy systems,” *Proceedings of the International Conference on Power Electronics and Drive Systems*, no. May 2014, 2007.

[45] V. Yaramasu, B. Wu, P. C. Sen, S. Kouro, and M. Narimani, “High-power wind energy conversion systems: State-of-the-art and emerging technologies,” *Proceedings of the IEEE*, pp. 740–788, 2015.

[46] H. Cai, W. Qi, Z. Xie, J. Huang, and Y. Liu, “Research on Construction Schemes and Applicable Scenarios for Flexible Direct-Current Electricity Collector Grids of Offshore Wind Farm Clusters,” *2019 Asia Power and Energy Engineering Conference, APEEC 2019*, pp. 291–295, 2019.

[47] S. Hardy, K. van Brusselen, S. Hendrix, D. van Hertem, and H. Ergun, “Techno-economic analysis of HVAC, HVDC and OFAC offshore wind power connections,” *2019 IEEE Milan PowerTech, 2019*, pp. 1–6, 2019.

[48] S. Chaithanya, V. N. B. Reddy, and R. Kiranmayi, “A narrative review on offshore wind power transmission using low frequency AC system,” *Proceedings of the 2017 International Conference On Smart Technology for Smart Nation, SmartTechCon 2017*, pp. 52–58, 2018.

[49] Siemens, “High voltage direct current transmission - Proven Technology for Power Exchange,” 2016.

[50] N. B. Negra, J. Todorovic, and T. Ackermann, “Loss evaluation of HVAC and HVDC transmission solutions for large offshore wind farms,” *Electric Power Systems Research*, vol. 76, no. 11, pp. 916–927, 2006.

[51] L. Lazaridis, “Economic Comparison of HVAC and HVDCSolutions for Large Offshore Wind Farms underSpecial Consideration of Reliability,” 2005, [Online]. Available: http://www.diva-portal.org/smash/record.jsf?pid=diva2:609080

[52] I. M. de Alegría, J. L. Martín, I. Kortabarria, J. Andreu, and P. I. Ereño, “Transmission alternatives for offshore electrical power,” *Renewable and Sustainable Energy Reviews*, vol. 13, no. 5, pp. 1027–1038, 2009.

[53] ABB, “HVDC Light. It’s time to connect,” *Abb Id No: Pow0038 Rev. 09*, pp. 1–64, 2017, [Online]. Available: https://search.abb.com/library/Download.aspx?DocumentID=POW-0038&LanguageCode=en&DocumentPartId=&Action=Launch

[54] O. Singh and S. K. Rajput, “Mathematical modelling and simulation of solar photovoltaic array system,” *International Conference on Research Advances in Integrated Navigation Systems, RAINS 2016*, 2016.

[55] X. H. Nguyen and M. P. Nguyen, “Mathematical modeling of photovoltaic cell/module/arrays with tags in Matlab/Simulink,” *Environmental Systems Research*, vol. 4, no. 1, 2015, doi: 10.1186/s40068-015-0047-9.

[56] M. M. Fouad, L. A. Shihata, and E. S. I. Morgan, “An integrated review of factors influencing the performance of photovoltaic panels,” *Renewable and Sustainable Energy Reviews*, vol. 80, no. May, pp. 1499–1511, 2017.

[57] A. Shukla, K. Kant, A. Sharma, and P. H. Biwole, “Cooling methodologies of photovoltaic module for enhancing electrical efficiency: A review,” *Solar Energy Materials and Solar Cells*, vol. 160, no. July 2016, pp. 275–286, 2017.

[58] N. A. Kamarzaman and C. W. Tan, “A comprehensive review of maximum power point tracking algorithms for photovoltaic systems,” *Renewable and Sustainable Energy Reviews*, vol. 37, no. February, pp. 585–598, 2014.

[59] P. P. Surya, D. Irawan, and M. Zuhri, “Review and comparison of DC-DC converters for maximum power point tracking system in standalone photovoltaic (PV) module,” *Proceeding - ICAMIMIA 2017: International Conference on Advanced Mechatronics, Intelligent Manufacture, and Industrial Automation*, pp. 242–247, 2018.

[60] H. Wang, L. Vinayagam, H. Jiang, Z. Q. Cai, and H. Li, “New MPPT solar generation implemented with constant-voltage constant-current DC/DC converter,” *Proceedings - 2016 51st International Universities Power Engineering Conference, UPEC 2016*, vol. 2017-Janua, no. 2, pp. 1–6, 2016.

[61] M. N. Ali, K. Mahmoud, M. Lehtonen, and M. M. F. Darwish, “An Efficient Fuzzy-Logic Based Variable-Step Incremental Conductance MPPT Method for Grid-Connected PV Systems,” *IEEE Access*, vol. 9, pp. 26420–26430, 2021.

[62] N. Priyadarshi, S. Padmanaban, J. B. Holm-Nielsen, F. Blaabjerg, and M. S. Bhaskar, “An Experimental Estimation of Hybrid ANFIS-PSO-Based MPPT for PV Grid Integration under Fluctuating Sun Irradiance,” *IEEE Systems Journal*, vol. 14, no. 1, pp. 1218–1229, 2020.

[63] D. Dong *et al.*, “A PV Residential Microinverter With Grid-Support Function: Design, Implementation, and Field Testing,” *IEEE Transactions on Industry Applications*, vol. 54, no. 1, pp. 469–481, 2018.

[64] F. Lu, B. Choi, and D. Maksimovic, “Autonomous Power-Source Regulation in Series-Connected Low-Voltage Microinverters,” *IEEE Journal of Emerging and Selected Topics in Power Electronics*, vol. 8, no. 2, pp. 1442–1453, 2020.

[65] S. Deshpande and N. R. Bhasme, “A review of topologies of inverter for grid connected PV systems,” *2017 Innovations in Power and Advanced Computing Technologies, i-PACT 2017*, pp. 1–6, 2017.

[66] M. Z. C. Wanik, A. A. Jabbar, N. K. Singh, and A. P. Sanfilippo, “Comparison on the Impact of 0.4 MW PV with Central Inverter vs String Inverter on Distribution Network Operation,” *2018 IEEE 7th International Conference on Power and Energy, PECon 2018*, pp. 162–167, 2018.

[67] B. Karanayil, S. Ceballos, and J. Pou, “Maximum Power Point Controller for Large-Scale Photovoltaic Power Plants Using Central Inverters under Partial Shading Conditions,” *IEEE Transactions on Power Electronics*, vol. 34, no. 4, pp. 3098–3109, 2019.

[68] C. D. Fuentes, C. A. Rojas, H. Renaudineau, S. Kouro, M. A. Perez, and T. Meynard, “Experimental Validation of a Single DC Bus Cascaded H-Bridge Multilevel Inverter for Multistring Photovoltaic Systems,” *IEEE Transactions on Industrial Electronics*, vol. 64, no. 2, pp. 930–934, 2017.

[69] E. Kabalcı, “Review on novel single-phase grid-connected solar inverters: Circuits and control methods,” *Solar Energy*, vol. 198, no. October 2019, pp. 247–274, 2020.

[70] V. Singh and A. N. Tiwari, “Study and Comparison of various types of Converters used for Solar PV: A Review,” *2018 International Conference on Power Energy, Environment and Intelligent Control, PEEIC 2018*, pp. 658–664, 2019.

[71] A. Smith and M. Tauer, “Getting to a Cleaner Future - Design Challenges and Solutions for Solar Inverters”.

[72] W. Xiao, “Review and simulation of flyback topology for module level parallel inverters in PV power systems,” *IEEE Region 10 Annual International Conference, Proceedings/TENCON*, vol. 2017-Dec., pp. 567–572, 2017.

[73] P. Somani and D. J. Vaghela, “Design of HERIC configuration based grid connected single phase transformer less photovoltaic inverter,” *International Conference on Electrical, Electronics, and Optimization Techniques, ICEEOT 2016*, pp. 892–896, 2016.

[74] M. A. Khan, A. Haque, and K. V. S. Bharath, “Control and stability analysis of H5 transformerless inverter topology,” *2018 International Conference on Computing, Power and Communication Technologies, GUCON 2018*, pp. 310–315, 2019.

[75] L. Zhang, K. Sun, Y. Xing, and M. Xing, “H6 transformerless full-bridge PV grid-tied inverters,” *IEEE Transactions on Power Electronics*, vol. 29, no. 3, pp. 1229–1238, 2014.

[76] W. Abd Halim, S. Ganeson, M. Azri, and T. N. A. Tengku Azam, “Review of multilevel inverter topologies and its applications,” *Journal of Telecommunication, Electronic and Computer Engineering*, vol. 8, no. 7, pp. 51–56, 2016.

[77] Q. X. Guan *et al.*, “An Extremely High Efficient Three-Level Active Neutral-Point-Clamped Converter Comprising SiC and Si Hybrid Power Stages,” *IEEE Transactions on Power Electronics*, vol. 33, no. 10, pp. 8341–8352, 2018.

[78] C. Li, S. Wang, Q. Guan, and D. Xu, “Hybrid Modulation Concept for Five-Level Active-Neutral-Point-Clamped Converter,” *IEEE Transactions on Power Electronics*, vol. 32, no. 12, pp. 8958–8962, 2017.

[79] Y. Wang and F. Wang, “Novel three-phase three-level-stacked neutral point clamped grid-tied solar inverter with a split phase controller,” *IEEE Transactions on Power Electronics*, vol. 28, no. 6, pp. 2856–2866, 2013.

[80] D. Floricau, G. Gateau, and A. Leredde, “New active stacked NPC multilevel converter: Operation and features,” *IEEE Transactions on Industrial Electronics*, vol. 57, no. 7, pp. 2272–2278, 2010.

[81] L. Zhang, K. Sun, L. Feng, H. Wu, and Y. Xing, “A family of neutral point clamped full-bridge topologies for transformerless photovoltaic grid-tied inverters,” *IEEE Trans. Power Electron.*, vol. 28, no. 2, pp. 730–739, 2013.

[82] K. Kumari, S. Mapa, and R. Maheshwari, “Loss analysis of NPC and T-Type three-level converter for Si, SiC, and GaN based devices,” *PIICON 2020 - 9th IEEE Power India International Conference*, 2020.

[83] K. Alluhaybi and I. Batarseh, “Review and Comparison of Single-Phase Grid-Tied Photovoltaic Microinverters,” *2018 IEEE Energy Conversion Congress and Exposition, ECCE 2018*, pp. 7101–7108, 2018.

[84] Y. Fang and X. Ma, “A novel PV microinverter with coupled inductors and double-boost topology,” *IEEE Transactions on Power Electronics*, vol. 25, no. 12, pp. 3138–3146, 2010.

[85] O. Abdel-Rahim, M. Orabi, and M. E. Ahmed, “Buck-boost interleaved inverter for grid connected photovoltaic system,” *PECon2010 - 2010 IEEE International Conference on Power and Energy*, pp. 63–68, 2010.

[86] W. Wu, J. Ji, and F. Blaabjerg, “Aalborg inverter - A new type of ‘buck in buck, boost in boost’ grid-tied inverter,” *IEEE Transactions on Power Electronics*, vol. 30, no. 9, pp. 4784–4793, 2015.

[87] B. Zhao, A. Abramovitz, C. Liu, Y. Yang, and Y. Huangfu, “A Family of Single-Stage, Buck-Boost Inverters for Photovoltaic Applications,” *Energies*, vol. 13, no. 17, 2020.

[88] K. K. Naik and N. Venugopal, “1kW Home Inverter Using Cascaded Current Fed Push Pull Converter and SPWM Inverter,” *2018 9th International Conference on Computing, Communication and Networking Technologies, ICCCNT 2018*, pp. 1–5, 2018.

[89] K. Alluhaybi, S. Member, and I. Batarseh, “Comprehensive Review and Comparison of Microinverters,” *IEEE Journal of Emerging and Selected Topics in Power Electronics*, vol. 8, no. 2, pp. 1310–1329, 2020.

[90] H. Hu *et al.*, “A three-port flyback for PV microinverter applications with power pulsation decoupling capability,” *IEEE Transactions on Power Electronics*, vol. 27, no. 9, pp. 3953–3964, 2012.

[91] H.-J. Chiu *et al.*, “A module-integrated isolated solar micro-inverter,” *IEEE Transactions on Industrial Electronics*, vol. 60, no. 2, pp. 781–788, 2013.